Marine Geophysical Researches (2003) 24:279–310
DOI 10.1007/s11001-004-2173-z

The Ionian Abyssal Plain (central Mediterranean Sea): Morphology, subbottom structures and geodynamic history – an inventory

W. Hieke[1,*], H. B. Hirschleber[2] & G.A. Dehghani[2]
[1]*Lehrstuhl für Ingenieurgeologie (formerly: Lehrstuhl für Allgemeine, Angewandte und Ingenieur-Geologie), Technische Universität München, Arcisstr. 21, D-80290 München, Germany;* [2]*Institut für Geophysik, Universität Hamburg, Bundesstr. 55, D-20146 Hamburg, Germany; (*Author for correspondence E-mail: werner.hieke@tum.de)*

Received 29 July 2004; accepted 05 August 2004

Key words: Ionian Abyssal Plain, Mediterranean Ridge accretionary complex, Messinian evaporites, tensional tectonics, thinned continental crust

Abstract

In order to understand the structure and evolution of the Mediterranean Ridge accretionary complex, it is necessary to understand the structure and history of its foreland. The Ionian Abyssal Plain is one of the varying types of foreland. The state of knowledge for that is presented. Its contour and detailed relief are described for the first time. Based on published and hitherto unpublished seismic data, information on the thickness of the Plio-Quaternary and on the Messinian evaporites are presented. Of particular interest are data concerning the pre-Messinian reflectors. They indicate a pattern of tilted blocks and horst-like features created in pre-Messinian time by tensional tectonics. Varying subsidence continued, however, during Messinian time and controlled the thickness of evaporites. At some places (e.g. Victor Hensen Seahill) vertical tectonics seem to be still active. The main tectonic structures of the Ionian Abyssal Plain are not related to the process of the present accretion and subduction at the Africa/Eurasia plate boundary but are pre-existing and should influence the internal structure of the Mediterranean Ridge which is still growing at the expense of the foreland. As a consequence of our structural evidence, we favour the following interpretation: the Ionian Abyssal Plain is not a remainder of the Jurassic Tethyan ocean but originated by extensive attenuation of continental crust.

Introduction

The ''Ionian Abyssal Plain'', located in the western Ionian Sea between the Calabrian Rise, the Mediterranean Ridge and the Medina Ridge has been named in the literature as follows:

- "Ionische Tiefsee-Ebene" (Pfannenstiel, 1960a, b), first map,
- "Messina Abyssal Plain" (Ryan and Heezen, 1965)
- ''Sicilia plain'' (Carter et al. 1971)
- ''Ionian bathyal plain'' (Morelli 1978)
- ''Ionian Abyssal Plain'' (The International Bathymetric Chart of the Mediterranean = IBCM, Intergovernmental Oceanographic Commission, 1981). Note that Ryan et al. (1970, fig. 5) named a northwestern area of the Hellenic Trench, off Zakynthos, ''Ionian Abyssal Plain''.
- Catalano et al. (2000, 2001): confusing mixture of undefined terms (Ionian Abyssal Plain, Ionian basin, Ionian ocean, Western Ionian Abyssal Plain, deeper abyssal plain, Eastern Ionian Abyssal Plain) for the area between the Malta and the Apulian Escarpments. In some cases, the term ''Ionian Abyssal Plain'' embraces the ''Calabrian accretionary wedge''.
- Polonia et al. (2002) use the term ''Messina foredeep'' (in relation to the Mediterranean Ridge development).
- The list of geographical names of undersea features (IHO/IOC, 1990) contains only the name ''Ionian A.P.'' without reference to the familiar ''Messina A.P.'' but with the remark ''*to be substituted in the later IBCM editions by Ionian basin*''. Due to the horizontal seafloor, the reali-

zation of that recommendation would be a mistake.

Up to now, little has been known about the recent shape and extension of the abyssal plain, its sediment pile, its subbottom geology and its geodynamic history. Therefore, the Ionian Abyssal Plain has often been a matter of speculations, particularly when considered in plate tectonic models.

In the generally accepted plate tectonic scenario, the IAP is part of the African Plate subducting beneath the Hellenic and the Calabrian arcs as well. At the subduction zone towards the east, the Mediterranean Ridge arises as an accretionary complex and the IAP constitutes one of the forelands. The detailed internal structure of the MR is still mainly unknown, due to the poor penetration. The nature of the already accreted part of the foreland should have strongly influenced the internal structure of the Mediterranean Ridge. Therefore, it should be helpful for the understanding of the entire area to know the nature of the foreland, in our case of the present IAP.

It is the aim of this paper to present an inventory of IAP data embracing older mostly unpublished observations, as well as those from recent cruises. Basing on this data set, a hypothesis of the geodynamic of the IAP will be presented.

Data source

The echosounding and/or seismic reflection data compiled in this publication have been collected during the following cruises: Chain 61 (1966), Meteor 17 (1969), Marsili (1970, 1971 and 1979), Meteor 50 (1978), Sonne 30 (1984), Valdivia 120 (1992, MEDRAC), Meteor 25/4 (1993, MEDRAC II), project IMERSE (1994), Meteor 40/1 (1997; MEDRAC III) and the Italian CROP project (1991–1994). The tracks of these cruises are presented on Figure 1. For gravity and magnetics, our data (cruises Valdivia 120, Meteor 25/4 and 40/1) have been combined with various older data available from the GEODAS data bank. Some data have already been published: Finetti and Morelli (1973; Marsili), Hinz (1974; Meteor 17), Avedik and Hieke (1981; Meteor 50), Finetti (1981 and 1982; Marsili), Hieke and Wanninger (1985; Sonne 30), Hirschleber et al. (1994; Valdivia 120), Hartmann (1995; Valdivia 120), Hieke et al. (1998, Valdivia 120 and Meteor 25/4), Hieke and Dehghani (1999; Valdivia 120, Meteor 25/4 and 40/1), Catalano et al. (2000 and 2001; CROP), Reston et al. (2002; IMERSE) and Polonia et al. (2002; Marsili).

Data collected during a period of almost 30 years are different in quality, mainly in the positioning. For a better evaluation of the precision, Table 1 indicates the systems for positioning, echosounding and seismic reflections as well as gravity and magnetics (only cruises Valdivia 120, Meteor 25/4 and 40/1). In spite of technical progress, the older data contribute as well to the picture of the IAP which is presented in this publication.

Morphology

Contour and area

The International Bathymetric Chart of the Mediterranean (IBCM, Intergovernmental Oceanographic Commission, 1981) suggests that the plain is contoured by the 4000 m isobath. The deepest point indicated is 4140 m (corr.).[1] The complete and exact shape of IAP is still unknown. This might be the background for the suggestion to substitute the correct term ''abyssal plain'' by the unprecise ''basin'' (IHO/IOC, 1990).

The characters of the borders of IAP are influenced by varying sedimentary and structural peculiarities which make a uniform definition difficult. We defined the borders at those points of the echosounder lines where the horizontal, slightly wavy or slightly raised seafloor changes to a steeper slope or even to a break of the slope (tracks on Figure 1). From that a preliminary and incomplete shape of IAP has been derived (Figure 2).

The Calabrian Rise and Mediterranean Ridge borders are relatively well documented whereas data from the western corner, the western part of the Medina Ridge border and the northeastern corner are rare. The quality of the navigation varies, and is worst in the northeastern part of the Calabrian Rise side.

The IAP is triangular as directed by the orientations of Calabrian Rise, Mediterranean Ridge and Medina Ridge. The area is roughly estimated to 5000 km^2. Appearance and orientations of the rim sections vary considerably in detail according

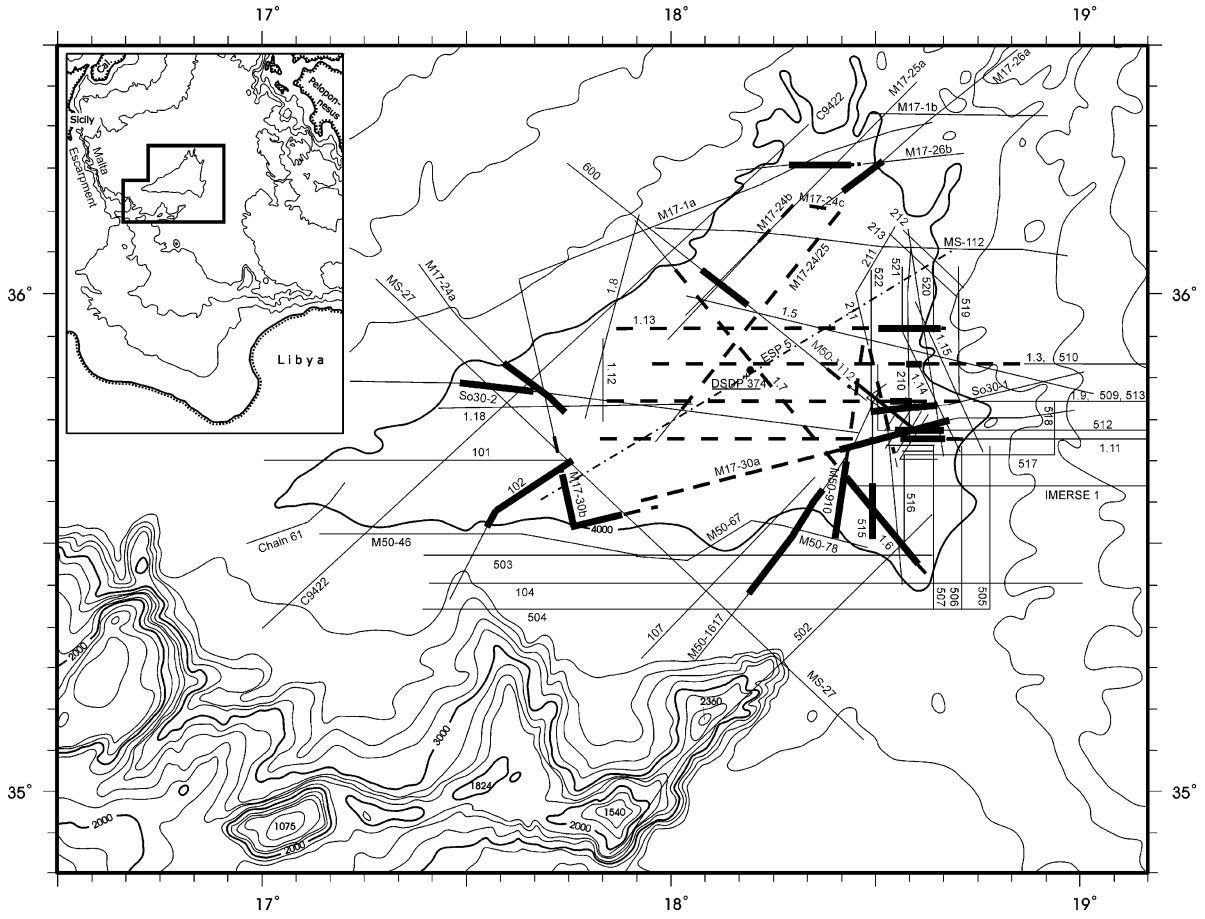

Figure 1. Bathymetric map (IBCM) of Ionian Abyssal Plain area with ship tracks and positions of ESP 5 (De Voogd et al., 1992) and DSDP Site 374. Track identification: 1.3–1.18 = Valdivia 120 (1992); 502–600 = Meteor 25 (1993); 101–213 = Meteor 40 (1997). Bold lines: IAP rim features on Figure 3, arranged clockwise starting with A in the northwest. Dashed bold lines: SCS and MCS lines on Figures 4 and 6–11.

to the respective rise area. The geographical coordinates of the rim positions of Figure 2 are listed in Table 2.

Calabrian Rise side

Dominant features at the lower Calabrian Rise are subsymmetrical elevations rising 5–30 m above the general trend of the seafloor, often beginning as slight undulations of the almost horizontal floor of the abyssal plain (Figure 1, So30-2 and M17-24a; Figures 3a and b). In most cases, the elevations produce a detailed relief modifying the continuously rising slope of the Calabrian Rise (Figure 1, 600; Figure 3c). The general slope gradients vary between 0°30′ and 2°. Between about 17°45′ and 18° longitude, a smooth wavy rise without pronounced elevations extends in front of the continuously rising slope (Figure 2, position 5).

Mediterranean Ridge side

The situation in the northernmost part is quite similar with that of the Calabrian Rise side: pronounced elevations modify the general slope of the lower MR. Near the contact with Calabrian Rise and MR (Figure 1, M17-26b and M17-26a; Figures 3d and e; ship's positions not very precise), undulations of the plain seafloor can be observed as on the Calabrian side. The general slope gradients are very gentle (about 0°30′). Further in the south to about 35°51′ latitude (Figure 1, 1.13; Figure 3f), the slope gradients vary between 1°10′ and 2°20′; there, the occurrence of undulations is not proved. Between

Table 1. Data source.

Cruise	Year	Positioning	Echosounding	Reflection seismics	Gravimetry	Magnetics
Chain 61	1966	various		100,000 joule sparker; Bolt PAR 600 air gun		
Meteor 17	1969	Loran C	30 kHz Schelfrandlot 15 kHz sonar (both with stabilized resonator)	SCS streamer AQUATRONIX; 2–3 airguns à 0.16 l		
Marsili (MS-21 and MS-21 ext.)	1970	Loran C		MCS streamer, active length: 2400 m, coverage of data: 12-fold; Flexotir, 3 à 50 g dynamite		
Marsili (MS-27)	1971	Loran C		like Marsili cruise 1970		
Meteor 50	1978	INDAS (Loran C plus satellites)	30 kHz "Schelfrandlot" 15 kHz sonar (both with stabilized resonator)	SCS streamer, active length: 150 m; TWG water gun: 1.3 l		
Marsili (MS-112)	1979	Loran C		like Marsili cruise 1970		
Sonne 30	1984	MAGNAVOX satellite system	O.R.E 3.5 kHz			
Valdivia 120 (MEDRAC)	1992	GPS	ELAC 30 kHz	MCS streamer, active length 2400 m, coverage of data: 24-fold; Airgun array: 6 (0.3–3.0 l), total volume: 7.9 l	KSS 30	ELSEC 7704
CROP	1991–1994			MSC streamer, active length 4500 m; 45-fold coverage of data (Catalano et al., 2000)		
Meteor 25/4 (MEDRAC II)	1993	GPS	ATLAS Parasound		KSS 30	GEOMETRICS G 811
IMERSE	1994	GPS		MCS streamer, active length 4500 m; Airgun array: total volume 80 l (Reston et al., 2002).		
Meteor 40/1 (MEDRAC III)	1997	GPS	ATLAS Parasound		KSS 30	GEOMETRICS G 813

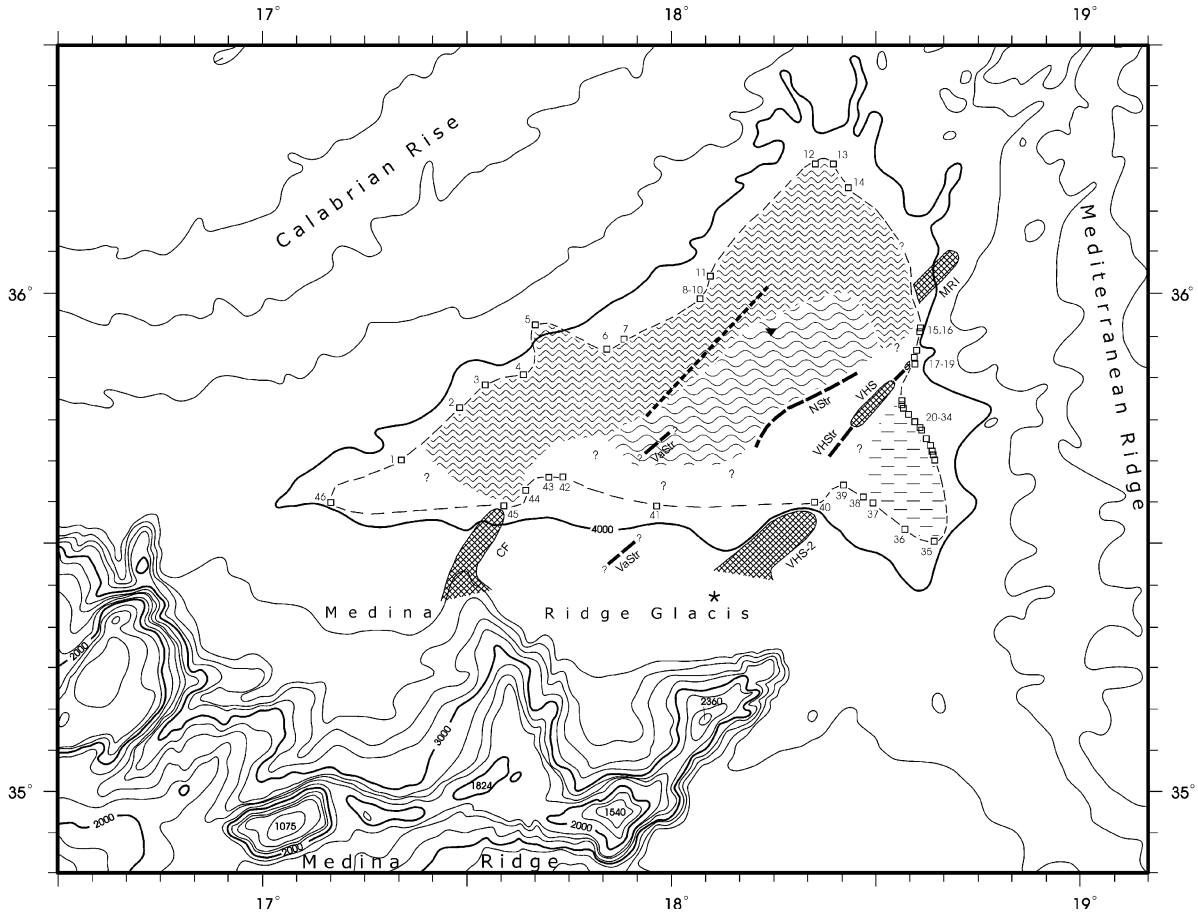

Figure 2. Bathymetric map (IBCM) of Ionian Abyssal Plain. Positions of the plain rim (numbers, see also Table 2) and approximate contour of the plain (thin dashed line). Cross hatched: relief elements not recorded in IBCM (CF = northern tip of the central finger of Medina Ridge; MRI = SW–NE oriented isobaths in the MR; VHS = Victor Hensen Seahill; VHS-2 = Victor Hensen Seahill 2).▼ = maximum depth of IAP. Bold dashed lines (long): subbottom structures (VHStr = Victor Hensen Structure, NStr = Nathalie Structure, VaStr = Valdivia Structure). Bold dashed line (short): axis of deepest position of TTL. Areas with waved lines (occurrence of "Undulation Zone" (Hinz 1974): undulations restricted to pre-TTL layers (wide screen) and affecting both pre- and post-TTL layers (narrow screen). Area with short lines = rising monoclines instead of undulations. * = position of subbottom prolongation of VHS-2 (Finetti and Morelli, 1972, fig. 11; 1973, fig. 29; Finetti, 1981, fig. 7; 1982, fig. 15 – see Hieke and Dehghani, 1999).

35°51′ and 35°43.5′ latitudes the slope rises in steps, forming "terraces" (Figure 1, 510, 513, So30-1, 512 and M17-30a; Figures 3g–k). The slope gradients vary between 0°30′ and 0°40′. Also the southernmost presented record (Figure 3l), again with rather subsymmetrical elevations, is characterized by the smooth gradient.

Medina Ridge side

Along this side the seafloor generally rises monotonously over a long distance (Figure 1, 515, 1.6 and M17-30b; Figures 3m, n and q) towards a broad W–E oriented shoulder in front of Medina Ridge ("Medina Ridge Glacis"; Hieke and Dehghani, 1999). A different type of rim occurs where "Victor Hensen Seahill 2" (VHS-2; Hieke and Dehghani, 1999) and the central finger of the Medina Ridge at 17°30′ E emerge. At VHS-2 the seafloor first rises slowly about 10 m above the plain level and then abruptly to 210 m above the plain (Figure 1, 910 and 1617; Figures 3o and p; Figure 2, positions 39 and 40). The situation at the central finger is similar. However, the northeastern foreland of the finger shows a small-scaled

Table 2. Geographic coordinates.

Data name	Coordinates		Water depth[a]	
Rim positions (locations see Figure 2)				
Against Calabrian Rise				
(1) M40-101	35°40.00′N	17°20.01′E	3950 m	
(2) 1.18	35°46.53′N	17°28.47′E	3960 m	*3968 m*
(3) So 30-2	35°48.99′N	17°32.53′E	3955 m	*3963 m*
(4) M 17-24a	35°50.0′N	17°37.1′E[b]	3958 m	*3966 m*
(5) M 17-30b	35°55.9′N	17°38.9′E[b]	3971 m	*3979 m*
(6) 1.12	35°53.23′N	17°49.82′E	3960 m	*3968 m*
(7) 1.8	35°54.46′N	17°52.80′E	3965 m	*3973 m*
(8) 1.6	35°59.35′N	18°03.40′E	3960 m	*3968 m*
(9) 1.7	35°59.47′N	18°03.62′E	3970 m	*3978 m*
(10) 1.5	35°59.29′N	18°02.60′E	3970 m	*3978 m*
(11) 600	36°01.44′N	18°05.71′E	3975 m	
(12) M 17-1a	36°15.1′N	18°18.6′E[b]	3958 m	*3946 m*
(13) M 17-26b	36°15.2′N	18°26.6′E	3958 m	
(14) M 17-26a	36°12.5′N	18°25.5′E	3955 m	
Against Mediterranean Ridge				
(15) 1.13	35°55.87′N	18°35.67′E	3968 m	*3976 m*
(16) 520/521	35°54.43′N	18°35.68′E	3970 m	
(17) 1.5	35°53.28′N	18°35.58′E	3970 m	*3978 m*
(18) 1.14	35°52.55′N	18°35.58′E	3969 m	*3977 m*
(19) 510	35°51.54′N	18°35.02′E	3978 m	
(20) 1.9	35°47.06′N	18°32.94′E	3970 m	
(21) 513	35°47.04′N	18°33.27′E	3972 m	
(22) So 30-1	35°46.15′N	18°35.19′E	3962 m	*3970 m*
(23) 202	35°46.50′N	18°34.98′E	3957 m	
(24) 201	35°46.44′N	18°33.66′E	3953 m	
(25) 203	35°45,00′N	18°35.46′E	3962 m	
(26) 512	35°43.76′N	18°34.81′E	3962 m	
(27) 205	35°43.32′N	18°34.98′E	3961 m	
(28) M 17-30a	35°43.3′N	18°35.4′E[b]	3965 m	*3973 m*
(29) 206	35°42,84′N	18°35.46′E	3962 m	
(30) 1.11	35°42.17′N	18°34.52′E	3953 m	*3961 m*
(31) 207	35°41.82′N	18°37.02′E	3963 m	
(32) 507/508	35°41.29′N	18°38.31′E	3958 m	
(33) 208	35°40.80′N	18°38.52′E	3958 m	
(34) 517	35°40.15′N	18°38.67′E	3960 m	
(35) 507	35°29.78′N	18°38.30′E	3950 m	
Against Medina Ridge				
(36) 516	35°31.03′N	18°34.00′E	3960 m	
(37) 515	35°34.80′N	18°29.52′E	3970 m	
(38) 1.7	35°34.79′N	18°28.67′E	3960 m	*3968 m*
(39) M 50	35°37.05′N	18°25.0′E[b]	3962 m	*3970 m*
(40) M 50	35°35.2′N	18°21.0′E[b]	3960 m	*3968 m*
(41) M 17-30a	35°34.5′N	17°58.0′E[b]	3957 m	*3965 m*
(42) M 17-30b	35°38.3′N	17°43.3′E[b]	3968 m	*3976 m*
(43) 102	35°37.6′N	17°40.6′E	3970 m	
(44) 102	35°35.8′N	17°36.8′E	3971 m	
(45) 102	35°33.2′N	17°33.8′E	3971 m	
(46) Chain 61	35°35′N	17°10′E[b]	?	

Table 2. Continued.

Data name	Coordinates		Water depth[a]
Other positions			
DSDP 374	35°50.87′N	18°11.78′E	4078 m corr.
MS-27 VHS-2 prolongation	35°24.4′N	18°06.0′E[b]	
So30/A	35°43.36′N	18°26.06′E	
513/A	35°47.04′N	18°17.80′E	
600/A	35°49.28′N	18°24.20′E	
660/B	25°49.72′N	18°23.52′E	

[a]See foot-note[2] in the text.
[b]Position not very exact.

relief which is the expression of subbottom structures (Figure 3r). Note that the central finger reaches farther to the north than indicated in the IBCM.

In summary, the morphological characteristics of the IAP rims differ: the slopes of Calabrian Rise and Mediterranean Ridge are complicated by elevations superimposed on the general rise or accentuating step-like ''terraces'', in contrast, towards the Medina Ridge the seafloor generally rises continuously and gently.

Bathymetry and relief

IAP is neither horizontal nor free of any relief. The exact bathymetry is difficult to ascertain due to (a) the diversity of sound velocities used for echosounding and (b) the recording scale. Therefore, the most recent data (Parasound of cruise Meteor 25/4, 1993) have been taken as the standard, and the older data have been adjusted by 8–11 meters[2].

In the southeastern part of the plain emerges the Victor Hensen Seahill (VHS; Hieke and Wanninger, 1985, and Figures 4a and 8). It is a 10.5 km long and 1.75–2.4 km wide elevation with four summits in water depths between 3660 and 3740 m. The greatest elevation of VHS above the plain is about 320 m. The four summits are arranged in a nearly straight line striking about 040°. In detail, the seahill shows a continuous change of the orientations of slope sections. These orientations are grouped as follows: (1) 013–027° with a mean of 017°, and (2) 064–085° with a mean of 072°. The general orientation of the seahill (040°) corresponds to the bisectrix of the angle between both orientations (Hieke and Wanninger, 1985).

About 5 km NE of VHS rises a subbottom structure above the seafloor (Figure 3g) at the rim of the plain. It belongs obviously to the same structure as VHS.

A second remarkable feature is a depression of about 5 m maximum depth and 3 km width northwest of the northeastern end of VHS (Figure 4b). Its slopes are asymmetrical (northwestern one steeper than southeastern one).

VHS separates the main part of the plain from the southeastern corner. The depth of the base of VHS is 4 m deeper in the northwest (3978–3979 m) than in the southeast (3974–3975 m) (several M25 tracks and Hieke and Wanninger, 1985). The maximum depth of the plain (3982 m) is recorded in a shallow axial depression with SW–NE orientation (Figure 2). From there, the seafloor rises generally towards the southeast, intensified by the 4 m step along the VHS axis. Southeast of VHS, the seafloor shows a depression of 2–3 m depth parallel to VHS (Figure 4e) before rising almost continuously up to water depths of 3970 m at the rim.

Towards NW the seafloor rises from the deepest area (3982 m) more or less continuously (Figures 3a and 3c). Towards the northeastern rim of the plain (track 521), the water depth decreases in wavy rises to 3967 m. There, it is difficult to define the boundary of the abyssal plain against the Mediterranean Ridge. For that part of IAP west of 18° longitude, echosounding data are insufficient for such a detailed bathymetry. On the Medina Ridge side, the seafloor seems to be stable at 3976 m along line M17-30b (Figure 3q) without any relief. Towards the western corner (line M40-101) the seafloor rises continuously to 3950 m.

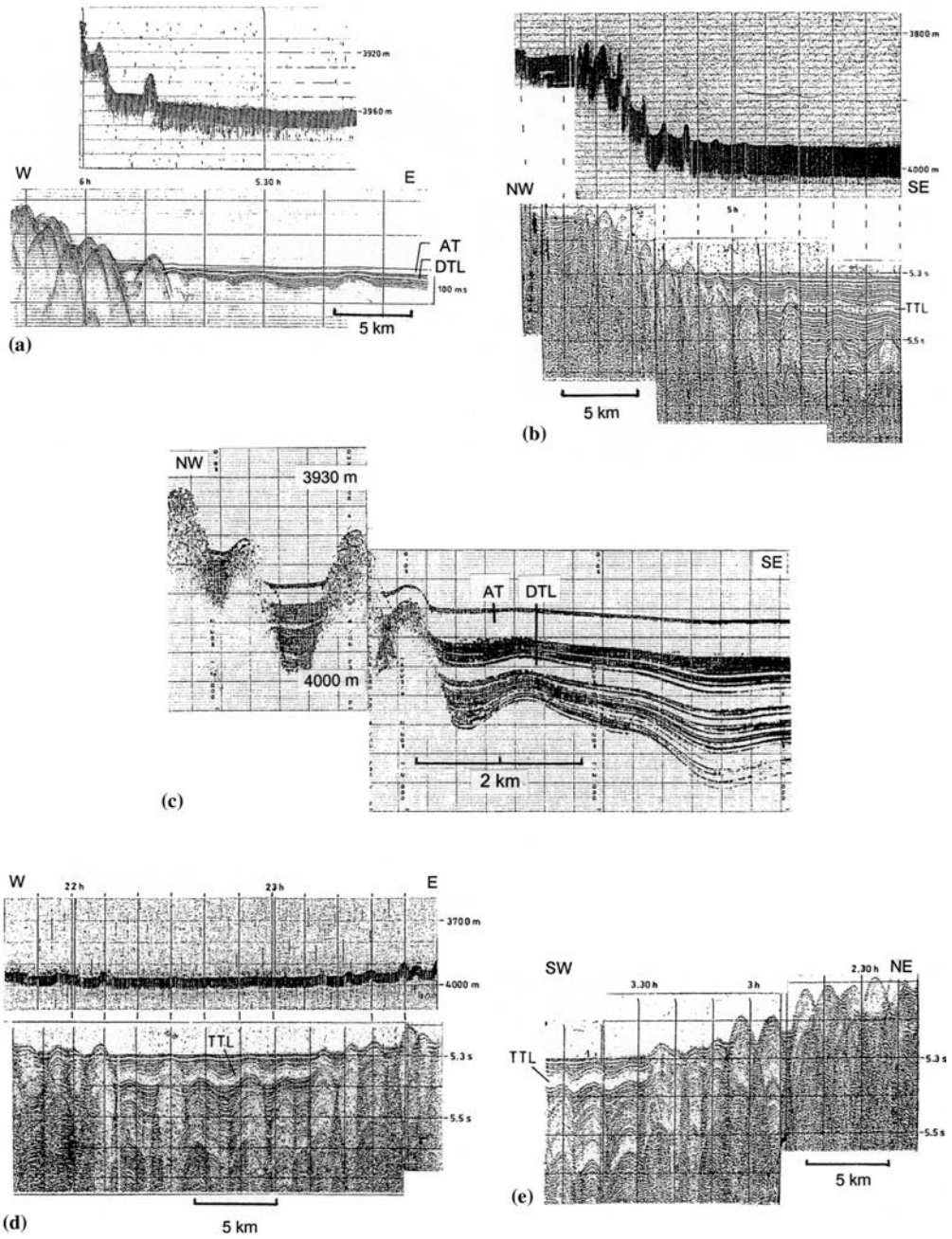

Figure 3. Examples of seafloor and subbottom situations at the rims of Ionian AP (Positions see Figure 1). *Calabrian Rise side:* **(a)**, corresponding echosounder and 3.5 kHz lines, Sonne 30; **(b)**, corresponding echosounder and SCS lines, Meteor 17, track 24a (identical with fig. 14 of Hinz, 1974). **(c)**, parasound line, Meteor 25, track 600; **(d)**, corresponding echosounder and SCS line, Meteor 17, track 26b. *Mediterranean Ridge side*: **(e)**, SCS line, Meteor 17, track 26a; **(f)**, Echosounder line, Valdivia 120, track 1.13; **(g)** and **(h)**: Parasound lines, Meteor 25, tracks 510 and 513; **(i)**, corresponding echosounder and 3.5 kHz lines, Sonne 30: **(j)**, Parasound line, Meteor 25, track 512, **(k)**, corresponding echosounder and SCS line, Meteor 17, track 30a; **(l)**, echosounder line, Valdivia 120, track 1.11. *Medina Ridge side*: **(m)**, Parasound line, Meteor 25, track 515; **(n)**, echosounder line, Valdivia 120, track 1.6; **(o)** and **(p)**, echosounder lines, Meteor 50, tracks 910 and 1617; **(q)**, echosounder line, Meteor 17, track 30b; **(r)**, Parasound line, Meteor 40, track 102. Seismic lines with depth scales in seconds TWT. AT = Augias turbidite; DTL = Deeper Transparent Layer; TTL = Thick Transparent Layer.

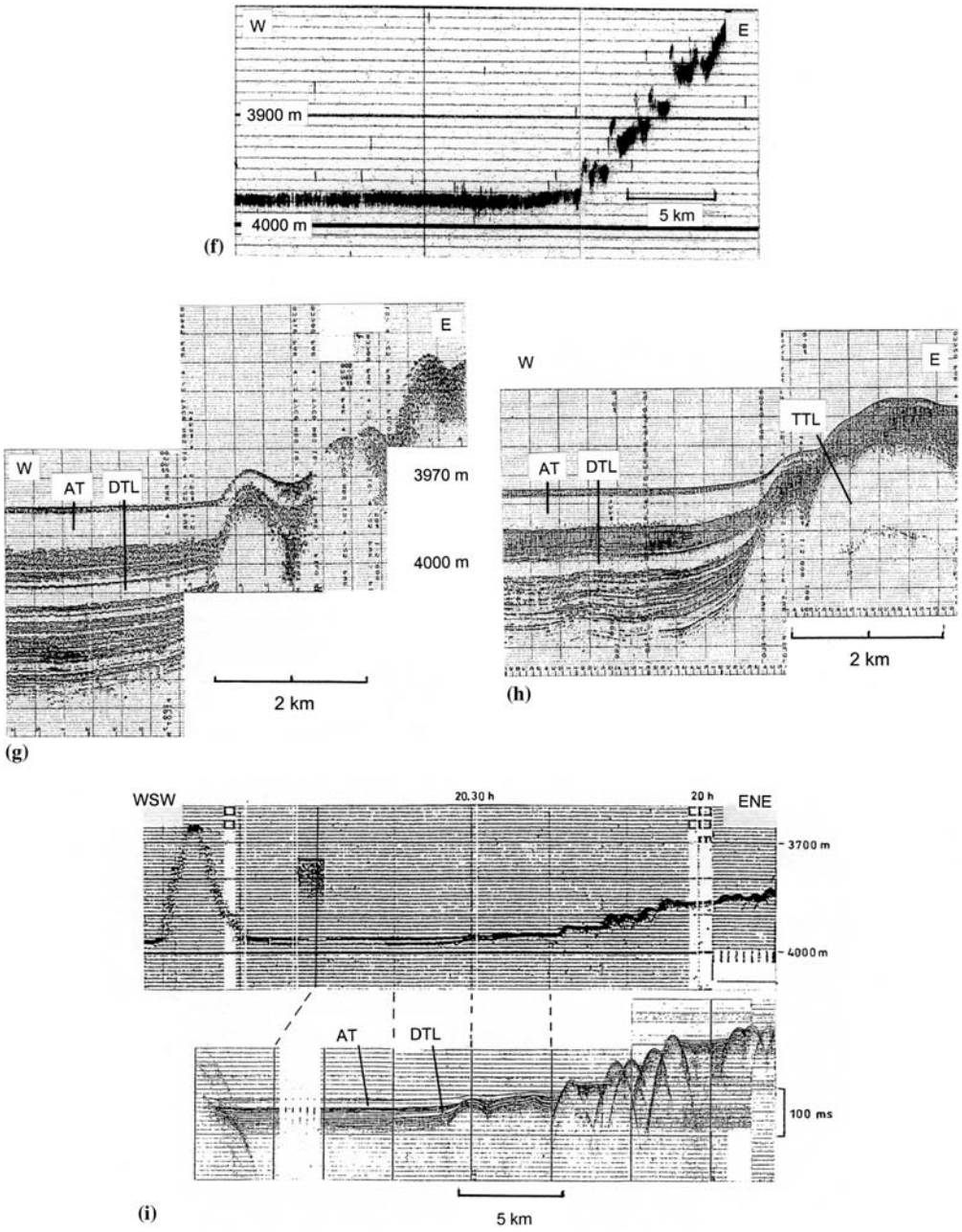

Figure 3. Continued.

The water depths of the plain rims vary. (1) Calabrian Rise side: increase from 3968 m (in the SW) to 3978 m (in the middle) and again decrease to 3968 m (in the NE). (2) Mediterranean Ridge side: variations between 3980 and 3970 m, not continuously but, with a general tendency of decrease from N to S. (3) Medina Ridge side: relatively stable between 3968 and 3970 m. (4) western corner: a continuous rise of the seafloor can be supposed.

As a summary of the general relief situation: the plain is not totally horizontal and at the same level. The greatest depth (3982 m) is recorded between VHS and Calabrian Rise (Figure 2).

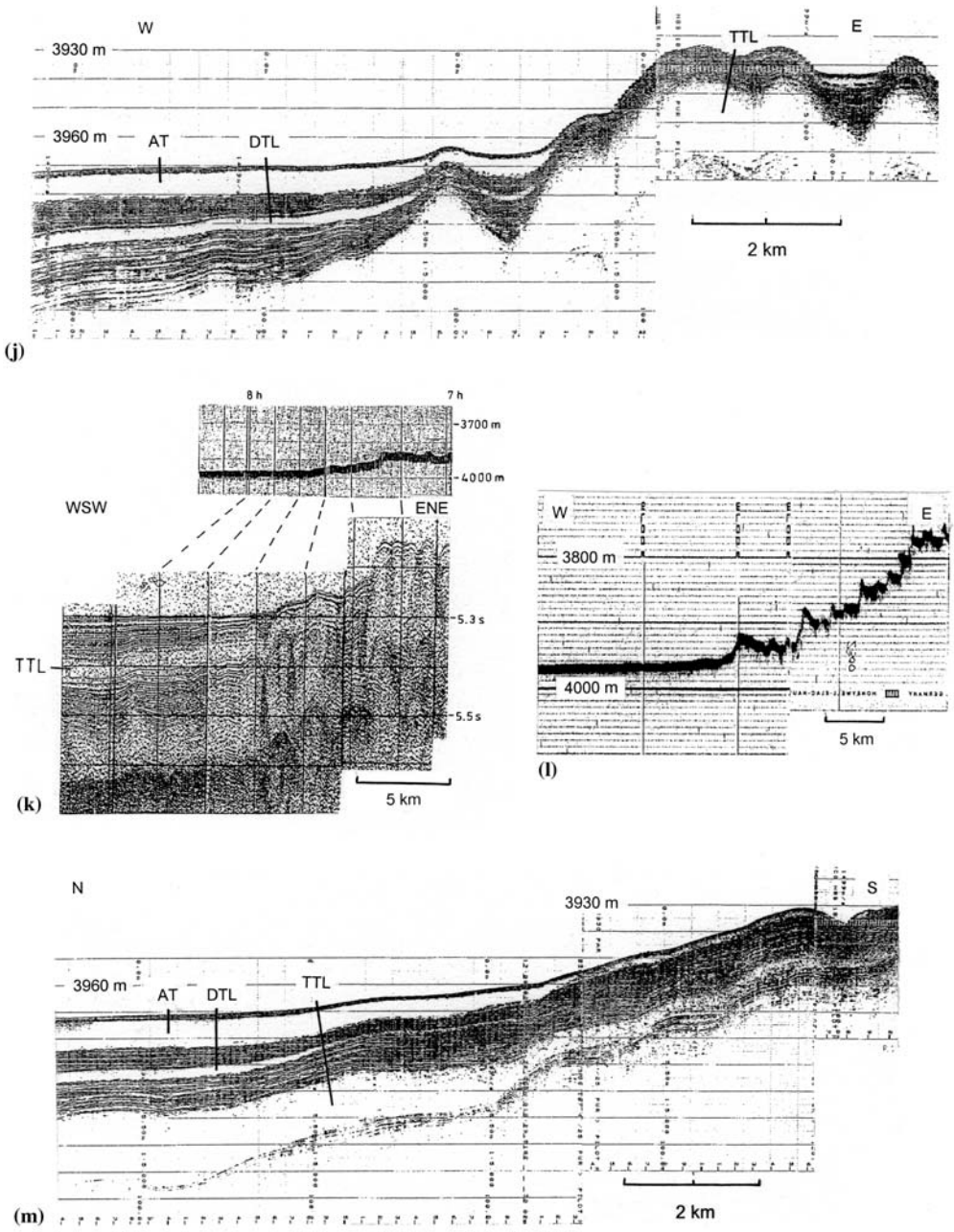

Figure 3. Continued.

The rims have varying water depths (3968–3978 m at the Calabrian Rise, 3970–3980 m at the Mediterranean Ridge and 3968–3970 m at the Medina Ridge sides). These observations result in an asymmetrical concave sea-floor pattern.

Sediments of the Ionian Abyssal Plain (IAP)

Direct information of the sediments comes from some piston cores and Deep Sea Drilling Project (DSDP) Site 374. DSDP Site 374, located at about the center of the plain (Figure 1), pene-

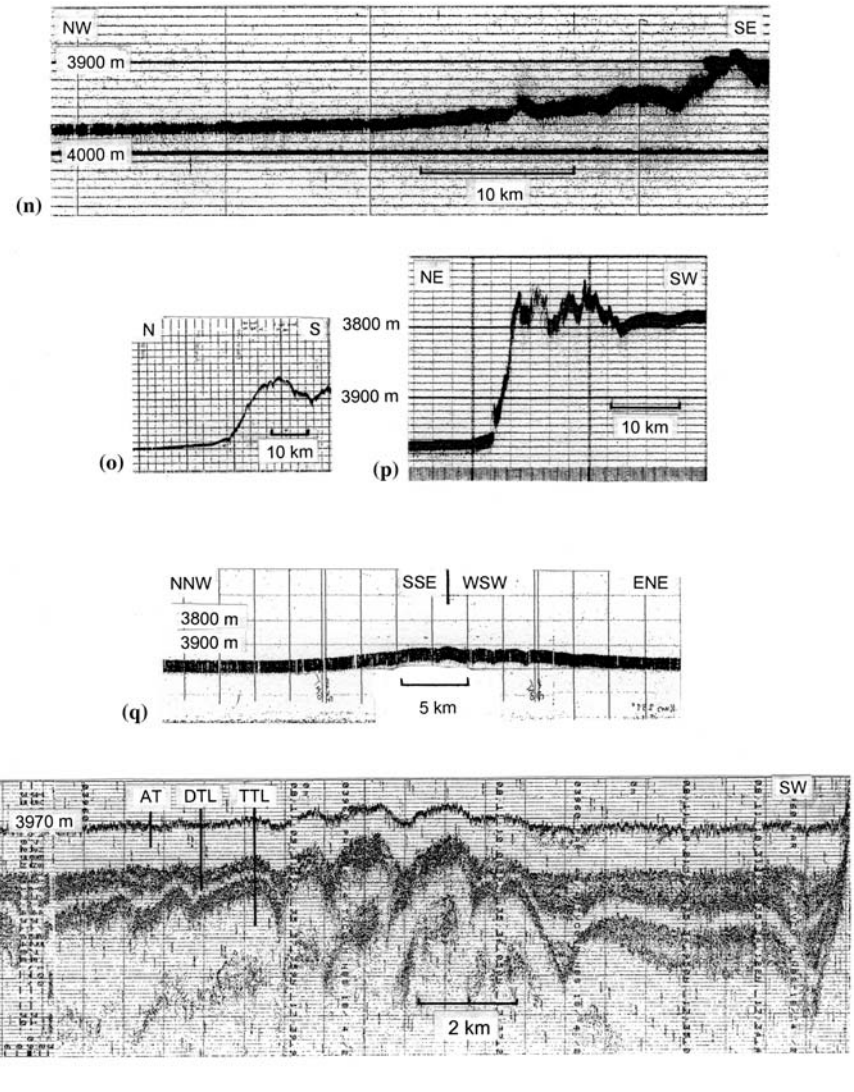

Figure 3. Continued.

trated the Plio-Quarternary sequence and over 80 m into the Messinian (Upper Miocene) evaporite formation. The thicknesses of Quaternary and Pliocene amount to 300 m and 60–80 m, respectively (Hsü et al., 1978). The corresponding mean sedimentation rates for Quaternary and Pliocene are about 14 cm $\times 10^{-3}$ years and about 2.1 cm $\times 10^{-3}$ years, respectively. The high Quaternary sedimentation rate is due to the dominance of turbidite deposits (Müller et al., 1978; Hieke, 2000; Hieke and Werner, 2000).

A turbidite with a maximum thickness of more than 12 m and a presumable age of 3500 years is recorded in piston cores (''homogenite'' – Kastens and Cita, 1981, Cita et al., 1984; ''Augias megaturbidite'' – Hieke, 1984).

The large number of publications with interpreted seismic lines suggests a high level of information on the pre-Messinian sequences. However, the stratigraphic interpretations are mainly based on extrapolations from neighbouring areas only. The streamer was often not long enough to calculate interval velocities from RMS data.

The largest part of published lines are repeated interpretations of MS lines obtained by the Osservatorio Geofisico Sperimentale, Trieste (e.g. Finetti 1981, 1982). A more substantial interpretation is that of seismic Flexotir lines

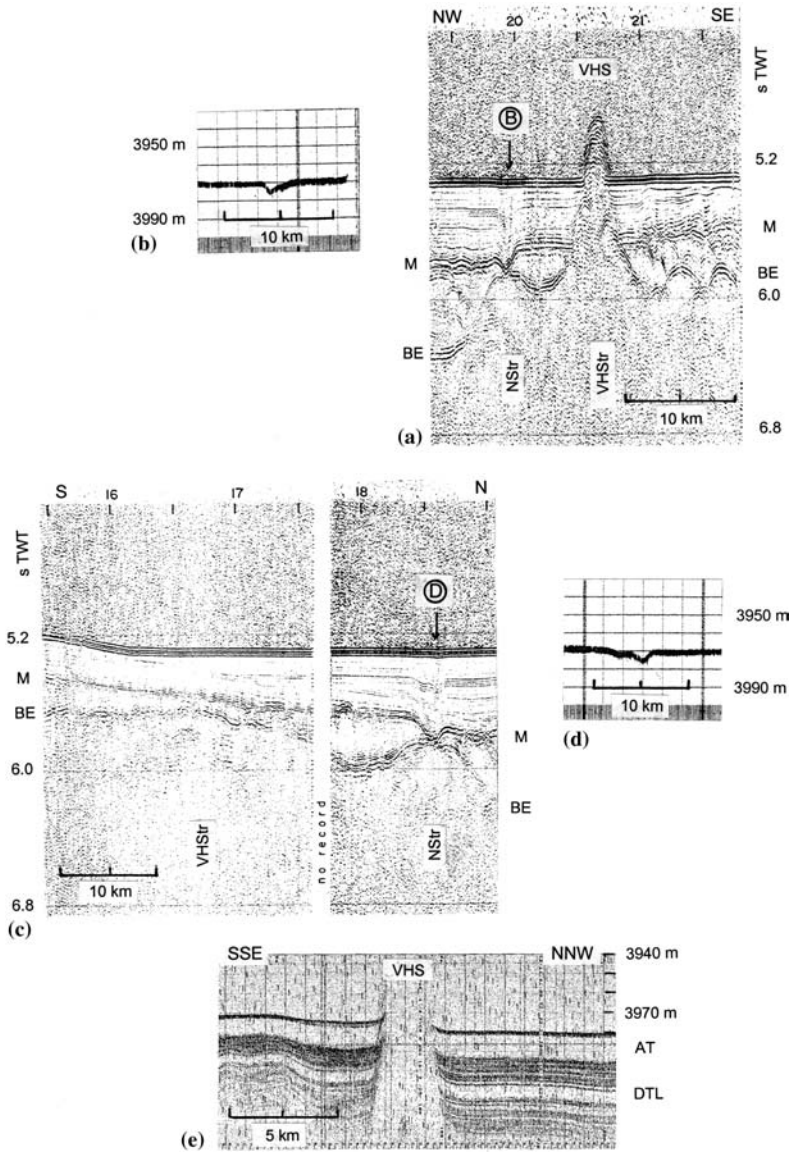

Figure 4. Seafloor and subbottom situations along Victor Hensen and Nathalie Structures. (**a**) and (**c**) from Avedik and Hieke (1981). (**a**), SCS line Meteor 50 (1978), track M50-1112 in Figure 1. (**b**) and (**d**): Echosounder records of the seafloor depression on top of NStr. (**c**), SCS line Meteor 50 (1978), track M 50-910 in Figure 1. (**e**), Parasound record Meteor 40 (1997), track 211A (not in Figure 1). AT = Augias turbidite; BE = base of evaporites; DTL = Deeper Transparent Layer; M = top of evaporites; NStr = Nathalie Structure; VHS = Victor Hensen Seahill; VHStr = Victor Hensen Structure.

MS-112 and GINA 4 by Casero et al. (1985, fig. 7) who were able to include knowledge from commercial wells on the Strait of Sicily platform. Casero et al. distinguish a terrigenous pre-evaporitic series of Tortonian to Messinian age, underlain by the "Gruppo Ragusano s.l." of Oligocene(?) to Serravallian age. Below this level, the authors provide no interpretation.

Subbottom information

Seismic reflection

About 30 years of seismic reflection studies have yielded data of various technics (subbottom profilers, single and multi-channel seismic equipments) and corresponding penetrations and

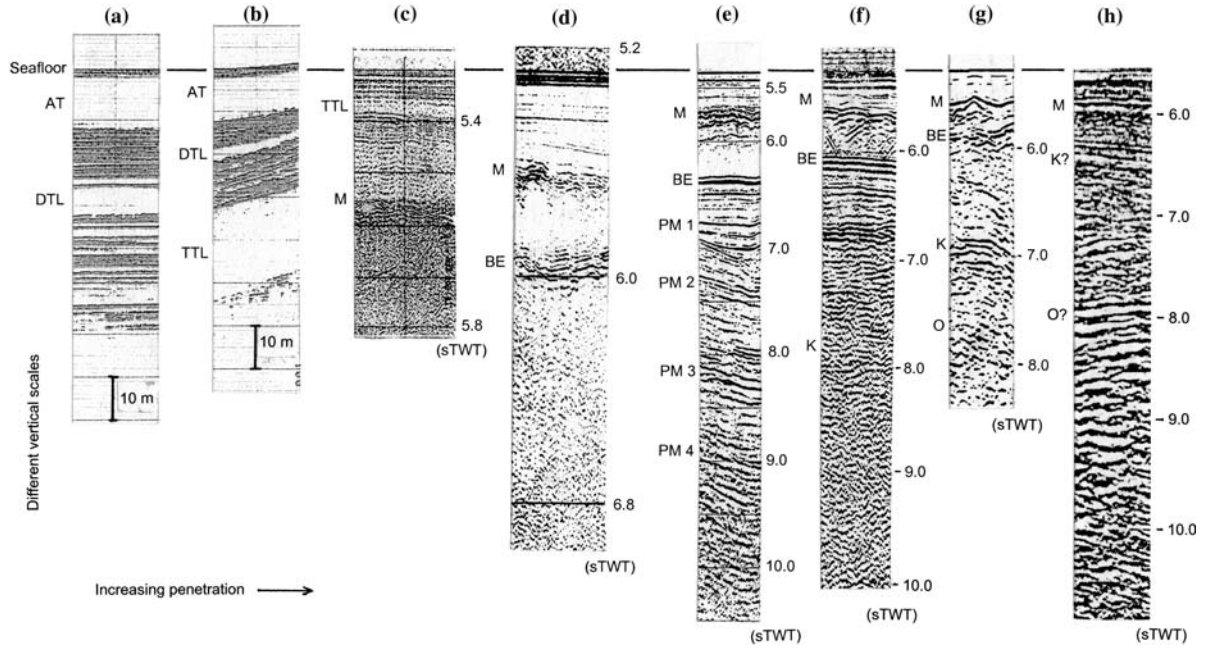

Figure 5. Examples of seismic resolution and stratigraphy depending on the methods. Note the different vertical scales. The sequence from (**a**) to (**e**) documents increasing penetration. The profiles (**f**) to (**h**) presents published stratigraphies with the respective original interpretations. (**a**) and (**b**), parasound (Meteor 25, tracks 513 and 515); (**c**), single channel seismic (Meteor 17, track 30a); (**d**), single channel seismic (Meteor 50, track 910); (**e**), multi channel seismic (Valdivia 120, track 1.7); (**f**), multi channel seismic MS-27 (Finetti and Morelli, 1973, fig. 32); (**g**), multi channel seismic IM-1 (Reston et al., 2002, fig. 10); (**h**), multi channel seismic C9422 (Catalano et al., 2001, fig. 7). AT = Augias turbidite, BE = base of evaporites, DTL = Deeper Transparent Layer, K = top of mesozoic carbonates, M = top of evaporites, Mo = Moho, O = Top of oceanic crust; PM1–PM4 = pre-Messinian reflectors; TTL = Thick Transparent Layer.

resolutions (Table 1). The data are presented here in three sections: (1) Plio-Quaternary with a high resolution section in the uppermost 30–60 m, (2) Messinian and (3) pre-Messinian.

Note that figures of seismic lines are erroneously indicated as ''Ionian Abyssal Plain'' on ''Ionian Abyssal Basin'' in following publications: Finetti (1981, MS-69, fig. 5; and MS-60, fig. 13); Finetti (1982, MS-60, fig. 18; MS-20, fig. 25; and MS-33, fig. 26) and Finetti et al. (1996, MS-33, fig. 2).

Seismic stratigraphy

The seismic stratigraphy is very detailed for the uppermost 30–60 m part of the sediment pile (subbottom profiler range). Below this interval, resolution decreases with increasing penetration. Figure 5 shows representative sections of our records with identified reflectors. Parts of profiles of Finetti and Morelli (1973), Catalano et al. (2001) and Reston et al. (2002) are included for comparison.

The subbottom profiler interval (Figures 5a–b) is characterized by numerous reflectors with short vertical distances which can be traced in many cases over the researched area. According to DSDP Site 374 all the reflectors are interpreted as the bases of turbidites (Müller et al., 1978). Conspicuous are three thick transparent levels: (1) the sedimentologically identified Augias megaturbidite (Hieke, 1984; Cita and Aloisi, 2000; Hieke and Werner, 2000); (2) the Deeper Transparent Layer, with 7 m maximum thickness and (3) the Thick Transparent Layer, with 35 m minimum thickness. DTL and TTL are interpreted in analogy to AT as megaturbidites as well. Their ages are very roughly estimated to 235,000 and 650,000 years, respectively (Hieke, 2000).

Records (Figure 5c) show also numerous parallel reflectors. TTL is the uppermost prominent interval identified in SCS lines. A conspicuous level recorded at about 100 m below the sea floor near the southern rim of the plain and outside is

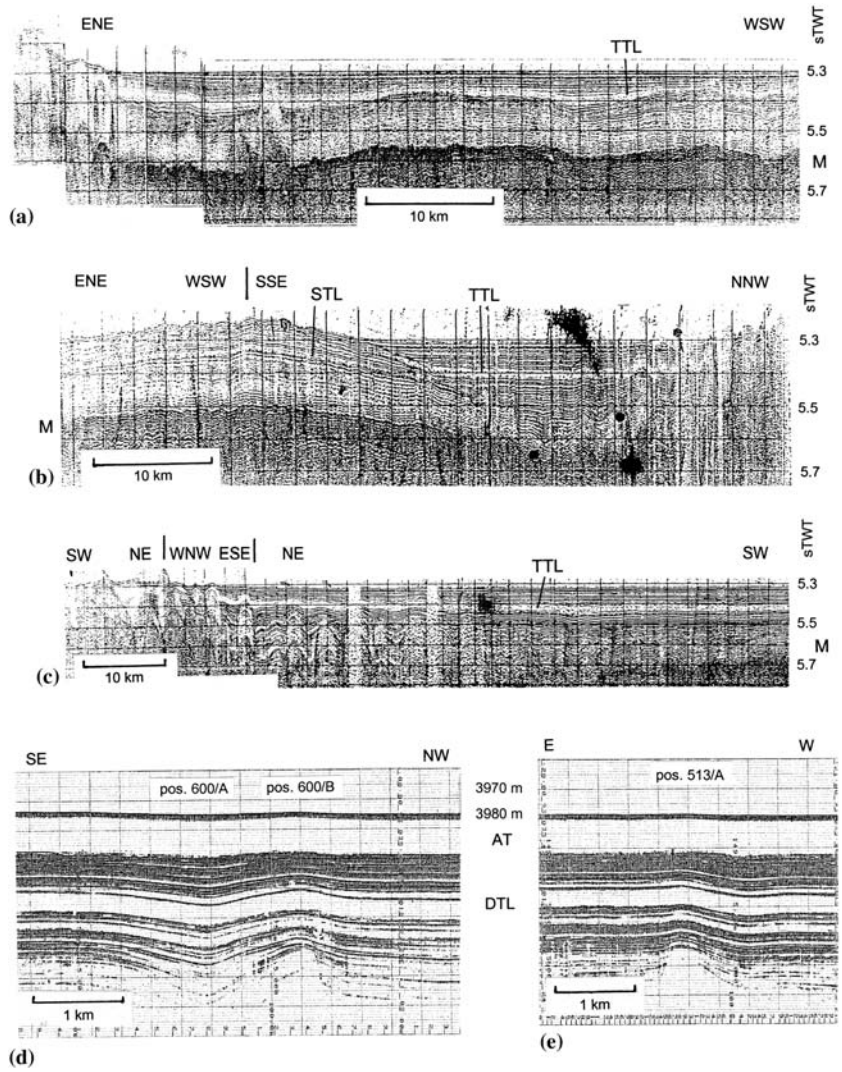

Figure 6. Subbottom situations. Single channel seismic lines from Meteor cruise 17 (1969): (**a**), M17-30a in Figure 1; (**b**), M17-30b in Figure 1; (**c**), M17-24b, c, and part of M17-24/5 in Figure 1. Parasound lines from Meteor cruise 25 (1993): (**d**), 600 in Figure 1, with positions 600/A and B; (**e**), 513 in Figure 1; with position 513/A. AT = Augias turbidite; DTL = Deeper Transparent Layer; M = top of evaporites; STL = Southern Transparent Layer; TTL = Thick Transparent Layer.

named "Southern Transparent Layer". It is clearly older than TTL and cannot be identified under the centre of the present plain (Figure 6b). Succeeding well identifiable horizons (Figures 5d and e) are reflector M (Ryan et al., 1970; top of Messinian evaporites) and BE reflector (base of evaporites).

Within the pre-Messinian, four prominent reflectors have been observed on seismic profiles of Valdivia cruise 120. They are named PM 1, PM 2, PM 3 and PM 4 (Figure 5e). Reflectors PM 1 and PM 3 can be correlated with the velocity/depth model of ESP 5 of de Voogd et al. (1992): PM 1 corresponds to S2, PM 3 corresponds to 2a (top of oceanic crust in the interpretation of de Voogd et al.).

In two sections of profile MS-27 of the Italian Marsili cruise, a reflector (K) at about 7.8 s TWT has been interpreted as top of the Mesozoic (Finetti and Morelli, 1973, fig. 32; Finetti, 1981, fig. 7; Finetti, 1982, fig. 14) and a second (Z) at about 9 s TWT as top of the basement (Finetti,

1981, fig. 7; Finetti, 1982, fig. 14). Reflector K corresponds with reflector PM 3.

The information given by Catalano et al. (2000, 2001) is confusing: seismic profile M3 crosses completely the Calabrian Rise (not the IAP) as also the larger part of profile C9422 does; only the southwestern part of the latter touches the western/northwestern rim of the IAP. From these lines, a seismic stratigraphy for the "Ionian deep basin" is derived by Catalano et al. (2001, fig. 8). The level indicated as top of "oceanic crust?" in profile C9422 at about 8 s TWT (l.c., fig. 7) corresponds in the crossing line MS-27 (Finetti and Morelli, 1973, fig. 32) with the above mentioned reflector K. Causing confusion, the same profile C9422 (= M22) is interpreted by Catalano et al. (2000, fig. 7) completely different: the top of the crystalline basement is situated at about 6 s TWT.

Reston et al. (2002) have published IMERSE profile 1 which crosses the MR and terminates in the southeastern corner of IAP. There the authors establish between their reflector B (at about 5.75 s TWT; corresponding with our BE) and reflector K (at about 7 s TWT; interpreted as top Mesozoic) their unit 3 (interpreted as Tertiary clastics; weak reflections; some Mesozoic?), and below K their unit 2 (interpreted as carbonates; strong, low frequency reflections; some clastics?). Strong reflectors like PM are not recognized.

The Plio-Quaternary interval

The 3.5 kHz/Parasound range displays a generally horizontal layering. The thicknesses of layers AT, DTL and the interval between them are fairly constant with about 12, 6 and 13 m, respectively, in the main part of the plain and 10, 5 and 11 m, respectively, in the southeastern corner. In detail and with increasing depth below seafloor the structural picture is much less monotonous:

(1) At a diffractional feature at position So30/A (which is the southwestern prolongation of the buried VHS, position see Table 2), DTL lies on the southeastern side few meters higher than on the northwestern one (Hieke and Wanninger, 1985, Figure 3G).
(2) Figure 6d shows a syncline/anticline feature which is most expressed in the subbottom with an amplitude of 15 m, but with only 1 m at the seafloor.
(3) An anticline 50 m below the seafloor (Figure 6e) flattens increasingly to a slight monocline at the seafloor.

The isolated features (2) and (3) are connected with Nathalie Structure in the deeper subbottom (see Section "The Messinian interval").

(4) Near the centre of the IAP (Figures 3b and 6c), small undulations affect only seismic layers just above reflector M. Approaching the northwestern and northeastern rims, undulations affect increasingly younger layers, cause slight bendings of the seafloor, and build distinct elevations (Figures 3a–e and 6c). The amplitude within each doming decreases vertically (approaching the seafloor). In this frame, the thicknesses of AT and DTL decrease to 9 and 5 m just before the rim and 5 and 2 m, respectively, outside the plain (Figure 3c). These features were called "Undulation Zone" by Hinz (1974). Its distribution is sketched on Figure 2.

Layering in the southeastern corner of the plain differs considerably. Towards MR, there exists no undulation but a pattern of rising monoclines of the layers and corresponding seafloor steps (Figures 3h, i and k).

Similar slight monoclinal bendings are observed towards the Ionian Gap (Figure 3m). There the thickness of AT decreases according to the rising seafloor up to a water depth of 3930 m where its record disappears. The thickness of DTL decreases earlier (from 5 to 3 m at the rim), and its record ends at 3960 m present water depth.

Detailed information from the deeper part of the Plio-Quaternary interval is available from a few tracks only. TTL (thickness in the order of 35 m; Hieke, 2000) might have been reached in all the Parasound lines, but mostly without penetrating its basal reflector. TTL lies not horizontal but dips generally from the rim (minimum depth 5.34 s TWT) towards the centre of the plain (Figure 6). The axis of the largest depth below seafloor (5.42 s TWT) coincides with the position of the maximum depth of the seafloor (Figure 2). TTL cannot be followed into the Calabrian Rise because of deficiency of penetration. Towards the Mediterranean Ridge, TTL is observed outside

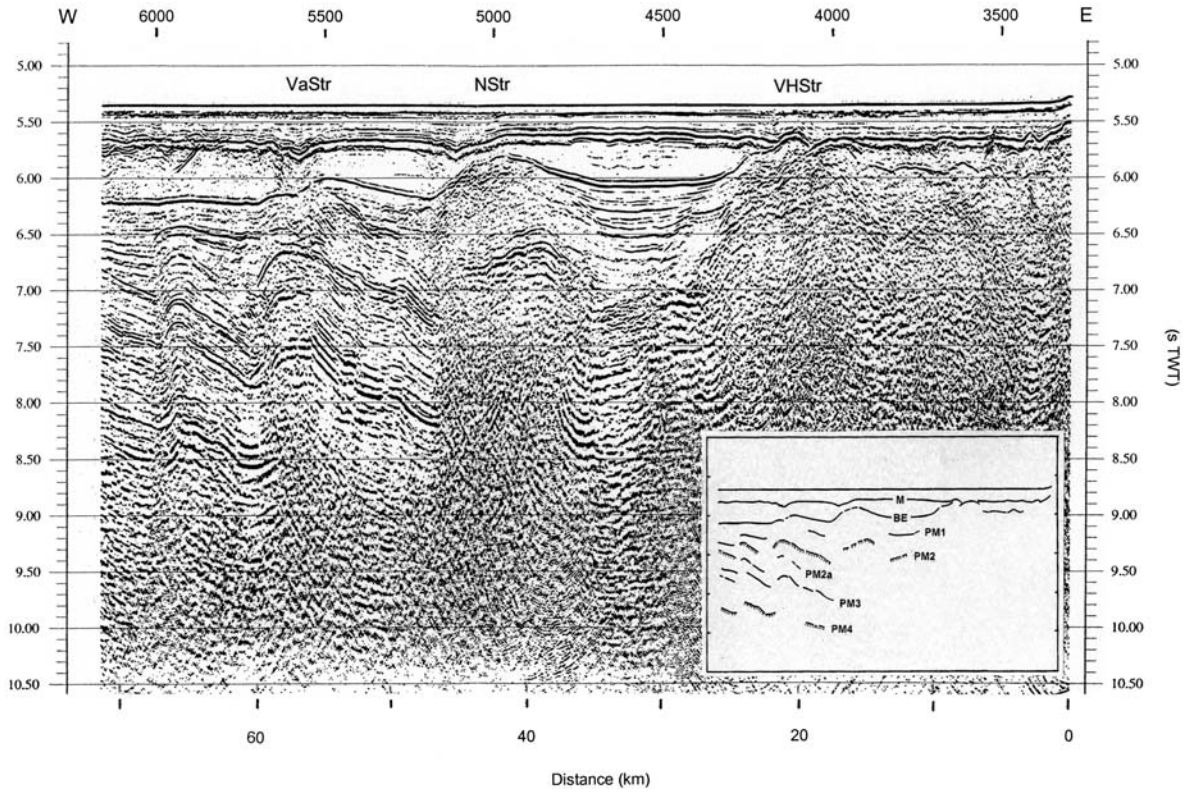

Figure 7. MCS line Valdivia 120 (1992), track 1.11. Upper horizontal indications are CMP (common measurement points). NStr, Nathalie Structure; VaStr, Valdivia structure; VHS, Victor Hensen Seahill; VHStr, Victor Hensen Structure. Interpretation insert: M, reflector M (top of Messinian evaporites); BE, base of evaporites; PM 1–PM 4, pre-Messinian reflectors.

the plain in the cobblestone-like features of track 513 (Figure 3h; top at 3962 m seafloor depth, thickness 28 m) and of track 512 (Figure 3j; 3945, 25 m) as well as in the monoclinal rise near the southeastern corner of the plain (Figures 3m and 6a).

A special situation is observed near the southern rim of the western part (Figure 6b). There, TTL rises abruptly towards the south and cannot be identified outside the plain. Since the seafloor is almost level, the thickness of the overlaying Quaternary sequence decreases considerably. In contrast to that, STL is recorded outside the plain, where the vertical distance to the seafloor is almost constant. STL dips under the plain and cannot be clearly identified at that position where TTL begins to rise.

Extraordinary features are V-shaped downbendings of the reflectors. They are best displayed on Figures 4a and c. The amplitude of the bendings decrease upward, and at the seafloor they result in the 5 m deep depression shown on Figures 4b and d.

The thickness of the Plio-Quaternary sequence increases generally in a small degree from SE to NW (Figures 7–11). Near the rim towards the Calabrian Rise, however, the thickness decreases abruptly (Figures 10 and 11) when the thickness of the evaporites increases (rise of reflector M).

The Messinian interval

The sequence of Messinian reflectors is interpreted in different ways. Hsü et al. (1978, p. 194) distinguish on seismic line OD 22 two layers and interpret them as ''upper evaporites'' and ''salt layer''. Kastens et al. (1992) assume a tripartition of the evaporite sequence under the Ionian Sea, which is documented by seismic records only for the western Mediterranean (Montadert et al.,

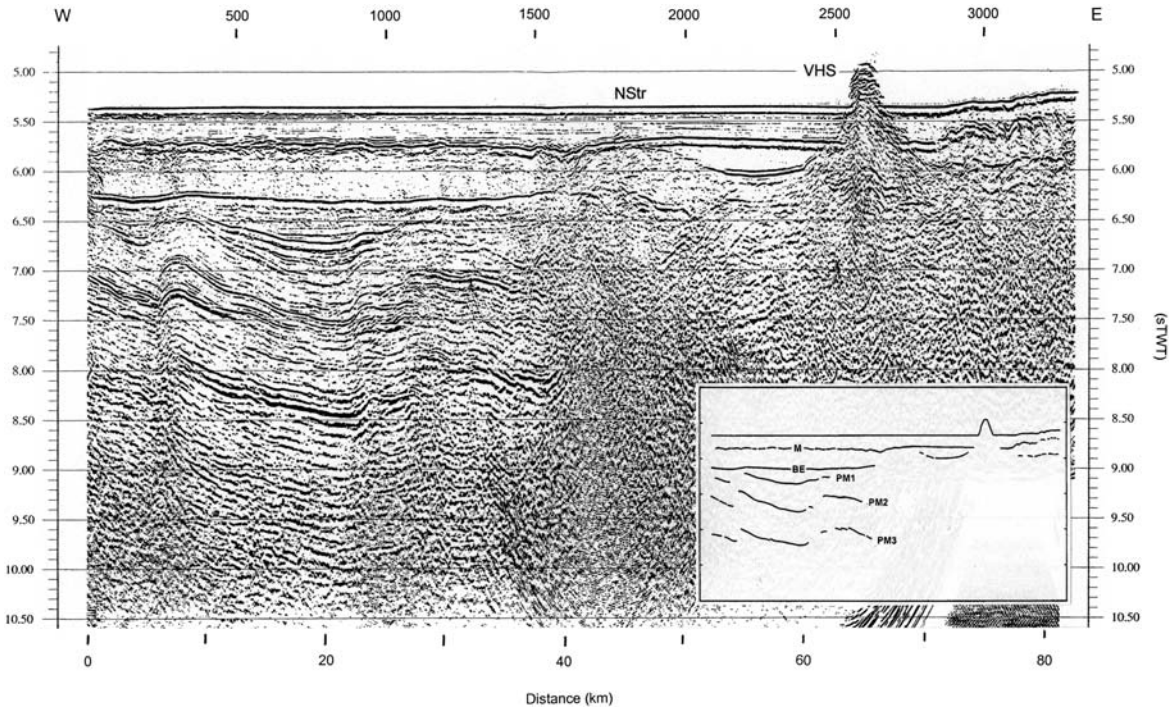

Figure 8. MCS line Valdivia 120 (1992), track 1.9. Abbreviations see Figure 7.

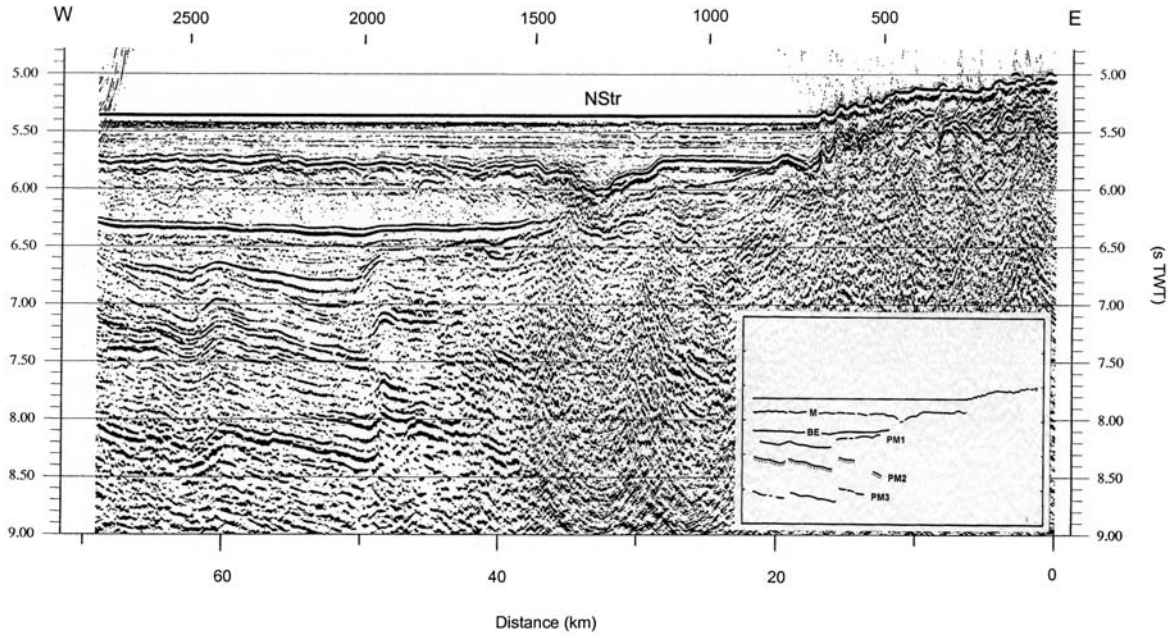

Figure 9. MCS line Valdivia 120 (1992), track 1.3. Abbreviations see Figure 7.

1978). De Voogd et al. (1992) subdivide the evaporites into two layers due to different velocities. On the seismic records presented in this paper, the Messinian interval shows only scarcely internal reflectors. A bipartition can be observed tentatively on Figures 7–11.

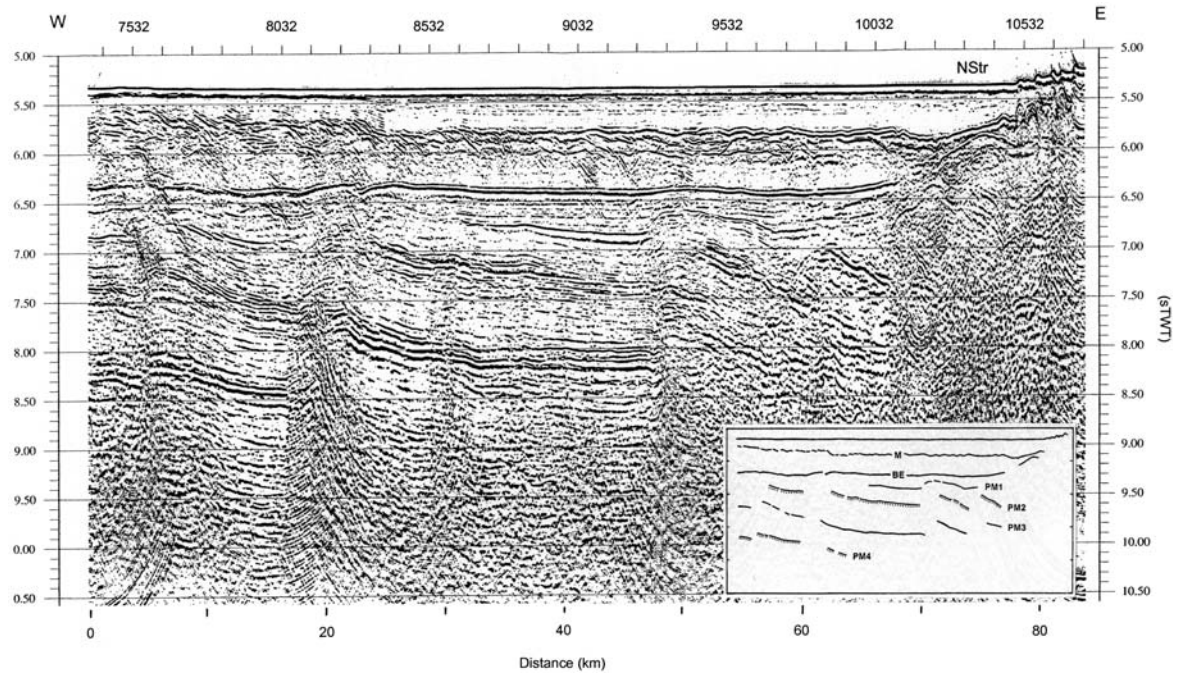

Figure 10. MCS line Valdivia 120 (1992), track 1.13. Abbreviations see Figure 7.

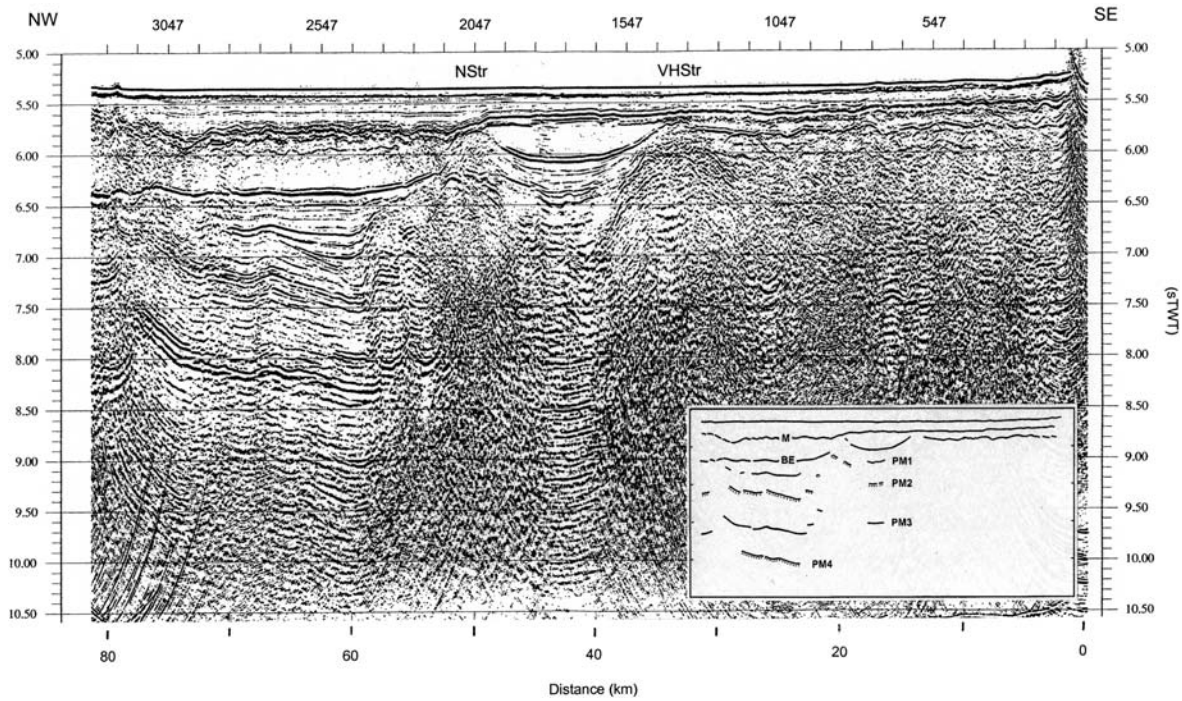

Figure 11. MCS line Valdivia 120 (1992), track 1.7. Abbreviations see Figure 7.

Reflector M lies generally horizontal. BE reflector is recorded mainly subparallel with M but in different depths below M. Exceptions are: (1) In Figure 7 (CMP 5200-5500) BE dips towards the E and is thus subparallel to deeper reflectors. (2) Considerable ''domings'' of BE can be joined to

three elongated structures where pre-Messinian rocks stand up (Figure 2): Victor Hensen Structure = VHStr and Nathalie Structure = NStr (Hieke, 1978; Avedik and Hieke, 1981; Hirschleber et al., 1994) and one recorded during Valdivia cruise 120 in 1992. It is much less dominant than VHStr and NStr, well developed to some extent only in the southern part of IAP (Figure 7) and named now "Valdivia Structure" (VaStr).

Within VHS the BE reflector rises extremely and interrupts the level of reflector M (Figures 4a and 8). West of NStr, the depth of M is about 0.1 s TWT deeper than east of it (Figures 7–9, 11). The increase of depth of reflector M is connected with monoclines or V-shaped down-bendings of the Plio-Quaternary reflectors. Though generally horizontal, M is wavy in detail west of NStr.

Figures 7, 8 and 11 illustrate that upstanding pre-Messinian rocks ("thresholds") bound "basins" in which variable maximum thicknesses of evaporites have accumulated. The respective maximum thickness of basins increases correspondingly with the depth of reflector M from SE to NW (the deeper reflector M, the thicker the underlaying evaporites). The maximum thickness of the evaporites in the southeastern corner is only one third of that in the area NW of NStr.

The primarily relatively low thicknesses on the thresholds have been reduced obviously often by a subsequent dissolution of evaporites, which produced V-shaped down-bendings. It is conspicuous that the "V"s are situated asymmetrically above the thresholds, according to the step-wise increase of the depth of reflector M.

Near the rim towards Calabrian Rise, the thickness of evaporites increases abruptly by rising of reflector M whereas the BE reflector stays almost horizontally (Figures 10 and 11).

The Pre-Messinian interval

In contrast to the previously described units, the pre-Messinian interval shows a more varying and dynamic picture.

Beneath the "domings" of BE, no (VHStr) or only a few reflectors (NStr) can be recognized. Between VHStr and NStr, the not fully discernible reflector sequence seems to display a concave, slightly asymmetrical feature (Figures 7 and 11). West and northwest of NStr, the sequence shows an asymmetrical pattern with eastward or southeastward dipping. The reflectors are jointly interrupted and antithetically tilted several times, producing a repetition of similar units. Comparable easterly dipping pre-Messinian reflectors are observed in the northeastern corner of IAP in profile MS-112 (Polonia et al., 2002, fig. 4).

The vertical distance between the reflectors is rather constant in the PM2/PM3 and PM3/PM4 intervals. PM1 is mostly dipping less than PM2 which results in a wedge-like increase of the PM1/PM2 interval thickness from the west (northwest) to the east (southeast) (best displayed in Figure 7). More conspicuous is the thickness variation of the BE/PM1 interval between the dominantly horizontal BE and the dipping PM1 reflectors.

The antithetical displacements of the PM reflectors are normally not paralleled by that of BE reflector. The exception is VaStr (Figure 7) where the high position of the reflector sequence coincides with a westward declining of BE and a V-shaped down-bending of reflector M. East of that exceptional VaStr, there is one more exception: the BE reflector dips towards the east (parallel with the underlying PM1).

Finetti (1982, fig. 14) has interpreted in MCS line MS-27 around 35°40′N and 17°45′E some lenticular reflector groups as volcanic layers indicating volcanic activity in pre-Messinian Miocene time. They correspond with the toe of the easternmost finger of Medina Ridge and the subbottom VHStr (both crossed in MS-27, Finetti, 1982, fig. 15; interpreted by Finetti as volcanic bodies as well). In Finetti's opinion, VHS (named "Marconi Seamount" by Finetti, 1982) is a large subcircular volcanic body. However, VHS is, as has been proved, of non-volcanic nature, and there are no arguments supporting the volcanic nature of the above mentioned features.

Inconsistent and confusing opinions are presented in the following publications: Catalano et al. (2001, fig. 7) give divergent and not data-based interpretations for a "half-lense-shaped body" in the southwestern segment of line C 9422: (1) a basaltic flow (which is not supported by magnetic anomalies, e.g. Finetti and Morelli, 1973, pl. XI, and IOC, 2000); (2) a deep-water clastic fan sourced from North Africa (which is

unrealistic because of the slightly rising toe of the Medina Ridge, as the relief shows).

The boundary "Tertiary/Mesozoic pelagic" of Catalano et al. (2001, fig. 7) corresponds in our lines 1.8 (crossing C9422) and 1.13 (Figure 10) with reflector BE.

The position of the top of the crystalline basement varies considerably if it is indicated at all. At the crossing of seismic lines M22 (=C9422) and M23, Catalano et al. (2000, pl. II and fig. 7) place it at about 6.6 s TWT. In contrast, Catalano et al. (2001, fig. 7) indicate that level at about 8 s TWT (base of the "clastics ?"). Moreover, lines M22 and M23 have been "calibrated" by Catalano et al. (2000) using the ESP data of de Voogd et al. (1992), however, there is no coincidence in the respective interpretations. So, the referred interpretations are highly questionable.

Seismic refraction

A first complete crust model based on seismic refractions was presented by Hinz (1974). It indicates the following profile:

4 km		water
0.5 km		Plio-Quaternary
1.5 km	vp = 4.0–4.5 km/s	Messinian evaporites
1.4 km	vp = 2.2 km/s	
4 km	Increasing vp from 5.0 to 6.8 km/s	
Below	Increasing vp from 6.8 to 8.5 km/s	

The velocity-depth model did not show a first order discontinuity between the crust and the mantle. A velocity of 8 km/s corresponds with a depth of about 19 km. The reinterpretation of Weigel (1974) results in three alternating models with a crust–mantle discontinuity at a depth of 16–17 km, where the velocity changes from 6.4 to 8.1 km/s. The crust thickness of this model is considered both by Hinz (l.c.) and Weigel (l.c.) to be between those of typically continental and oceanic ones and interpreted as developed by rifting or oceanization of a continental crust.

A second model was given by Makris et al. (1986). Along a profile from Sicily to IAP, data from three ocean bottom seismographs (OBS) were connected to a model with the boundary between 7.2 and 8.1 km/s at a depth of about 18 km northwesterly outside IAP (l.c., fig. 9). Unfortunately, the OBS from the abyssal plain itself had no data. Therefore, only unreversed data recorded at the rim of the basin are available. The extrapolated model results in a crustal thickness of 11 km for the IAP (6 km of sediments and 5 km of crystalline rocks). The crust–mantle boundary (Moho) was found as a first order discontinuity in 15 km depth, where the observed velocity changes from 7.2 to 8.1 km/s. Makris et al. believe that such a thin igneous crust can be of oceanic origin or severely stretched continental, intruded by upper mantle material.

Cloetingh et al. (1980) and Calcagnile et al. (1982) presented extreme interpretations of crust thicknesses of 35–40 and 35–51 km, respectively, inferred from Raleigh wave dispersion. Calcagnile et al. (l.c.) argue that the discrepancy with the model of Hinz (1974) may derive from a misinterpretation of a high-velocity layer within the crust (as generally postulated by Mueller, 1977) as the beginning of mantle material. Ferrucci et al. (1991) gave evidence of reduced crustal thickness in the middle of the Ionian basin, based on refraction seismic survey using OBSs.

The most recent survey was made in 1988 (Pasiphae cruise; De Voogd et al., 1992), carrying out expanding spread profiles (ESP). ESP 5 was measured in the IAP in SW–NE orientation. The velocity-depth model shows the top of the igneous crust at 9 km and the beginning of the mantle (8.5 km/s) at 17 km. From this, a thickness of the igneous crust of 8 km results. De Voogd et al. interpret the crust as oceanic.

During Valdivia cruise 120 (1992), some seismic refraction measurements were done by OBSs. The results confirm more or less the velocity-depth model of De Voogd et al. (l.c.) (Weigel, personal communication).

Gravity

Maps of free air and/or Bouguer gravity anomalies were published by Finetti and Morelli (1973), Morelli et al. (1975), IOC (1989) and Catalano et al. (2001) with different scales but similar information. In the free air gravity map, there are figured Medina Ridge as well as a SW–NE oriented chain of positive anomalies. The Bouguer maps show only one strong positive anomaly (+310 mGal; in the map of Catalano et al. +270 mGal). Its core trends SW–NE and

coincides with the VHS area. The escorting isolines outline a triangle which extends to the southeast as well.

The strong positive anomaly has been interpreted as follows:

- Finetti and Morelli (1973, p. 333): combination of thinning of the igneous crustal layer and of the upper Mantle density anomaly.
- Finetti (1981, p. 482): intermediate or oceanic crust with sialic fragments.
- Finetti (1982, p. 276): very consistent thinning of the Mesozoic sequence and uplifting of the basement, prominent volcanic activities with a seamount (meant is VHS).
- Boccaletti et al. (1984, p. 231): thinned crust, high-density intruded magmas, cooling of mantle material.

Gravity modelling supports the interpretation as a pre-Messinian tectonic structure probably constituted by shales and/or carbonates of Paleogene-Mesozoic age (Della Vedova and Pellis, 1989).

Our compilation of measurements made during cruises Valdivia 120 (1992), Meteor 25/4 (1993) and Meteor 40/1 (1997) as well as of data from GEODAS (Geophysical Data System for Marine Geophysical Data) gave a free-air gravity map, presented on Figure 12a. There, two areas of positive anomalies are most conspicuous: a W–E oriented chain at about 35° latitude (coinciding with the Medina Ridge) and a SW–NE oriented chain starting from the eastern finger of the Medina Ridge and including VHS. Hieke and Dehghani (1999) published free-air and Bouguer maps for the eastern part of the present Figure 12a. The Bouguer map is repeated as Figure 12b. It shows that the free-air anomaly coinciding with the eastern finger of the Medina Ridge is caused by the relief only, whereas the SW–NE oriented anomaly is caused by subbottom density anomalies.

The negative values in the northwestern part of Figure 12a indicate the lower slope of the Calabrian Rise as well as the relative flat area between IAP and Malta Escarpment. IAP does not become apparent in the gravity map.

Bouguer data for the western part of Figure 12 are not available since the quality of bathymetric data is not sufficient to correct the gravity data. Nevertheless, considering the general relief situation, distinct gravity anomalies are not to expect in that area.

Magnetics

An aeromagnetic survey presented by Vogt and Higgs (1969, fig. 2 and 6) shows residual magnetic anomalies with negative values, which coincide with the Medina Ridge. The authors assume that the anomalies may reflect young volcanism.

Also the map of total magnetic intensity of Finetti and Morelli (1973, pl. XI) shows anomalies which coincide with the Medina Ridge. They are much less spectacular than those along the Malta Escarpment where the occurrence of basalts has been observed (Scandone et al., 1981; Biju-Duval et al., 1982). Hieke and Dehghani (1999) demonstrated that the eastern finger of the Medina Ridge is characterized by strong magnetic anomalies (up to 180 nT), whereas no considerable anomalies can be identified in the area of VHS.

The map of magnetic anomalies (IBCM-M; International Oceanographic Commission, 2000) does indicate neither the VHS nor the eastern finger of the Medina Ridge by anomalies.

Our map of residual magnetic anomalies (Figure 12c) results from measurements of cruises Valdivia 120, Meteor 25/4, Meteor 40/1 and data of different source (GEODAS). It shows little correlation with the gravity map. The negative anomalies along 35°50′N might be the result of modern measurements contrasting to older ones (see tracks on Figure 12c).

VHS cannot be identified by an anomaly. Oceanic type magnetic anomalies have never been recorded.

Heat flow

A simplified heat flow map of the Eastern Mediterranean on the base of Čermak and Hurtig (1979) was published by Makris and Stobbe (1984). It shows mainly low heat flow values (<0.9 HFU $= 37.7$ mWm^{-2}) and a W–E oriented zone with values of 0.9–1.6 HFU ($=37.7$–67 mWm^{-2}) in the area north of the Medina Ridge.

Erickson et al. (1977) report a generally low average value (0.74 ± 0.30 HFU $= 31 \pm 12.6$ mWm^{-2}) in the Eastern Mediterranean and no

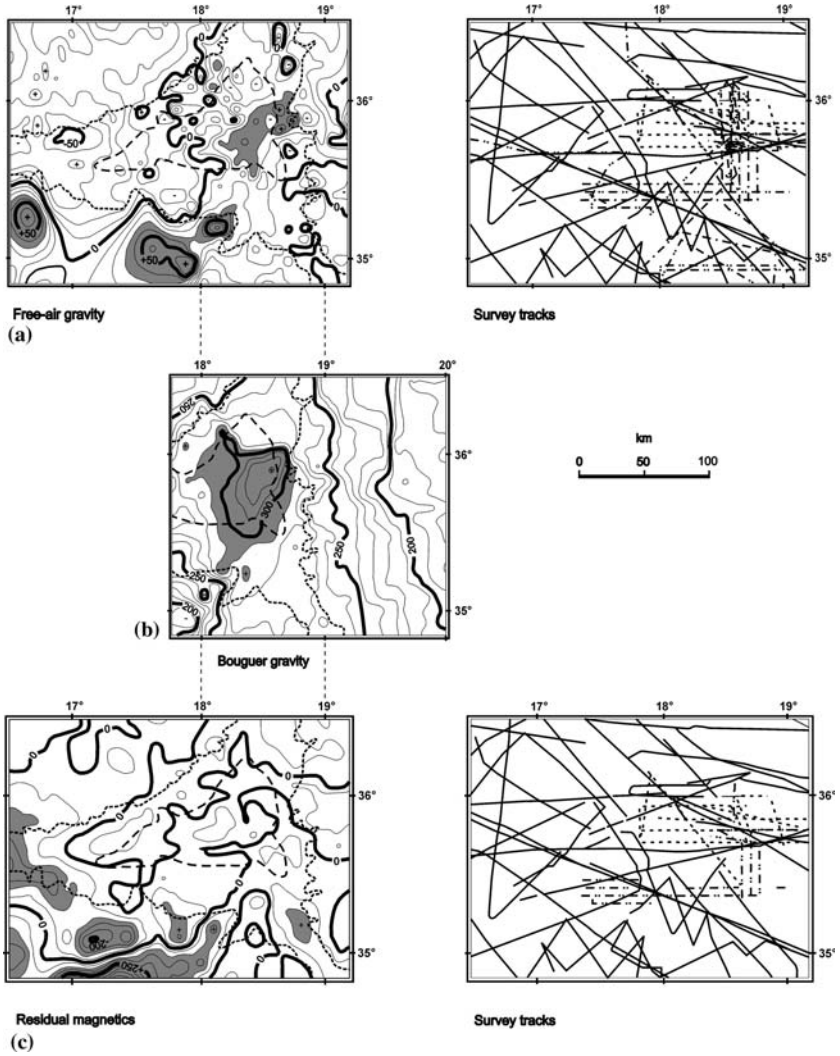

Figure 12. Maps of gravity and magnetic anomalies of the Ionian Abyssal Plain area and corresponding track charts. Relief information in the anomaly maps: long-dashed line = contour of the Ionian Abyssal Plain, short-dashed line = 3800 m isobath. Track maps: solid lines = data from GEODAS; dashed lines = data collected by the authors (Valdivia 120, Meteor 25 and Meteor 40). (**a**): Free-air gravity anomalies (based on the 1967 formula). Bold lines = 50 mGal intervals; thin lines = 10 mGal intervals; gray = areas with extreme positive values (exceeding + 30 mGal). (**b**): Bouguer gravity anomalies (Hieke and Dehghani, 1999, fig. 6). Gray = areas with extreme values (exceeding 190 mGal). Bouguer data for the western part of (**a**) are not available due to insufficient quality of bathymetric data. (**c**): Residual magnetic anomalies. For all measurements, there have been calculated the corresponding regional fields (using IGRF and DGRF, respectively) and subtracted from the total field. Bold lines = 250 nT intervals; thin lines = 50 nT intervals; gray = areas with extreme intensities (exceeding + 100 nT and −100 nT).

evidence for any regional heat flow anomaly associated with the Mediterranean Ridge, nor with the basin and trench provinces located north or south of it. In the central part of IAP a value of 0.80 ± 0.10 HFU (33.5 ± 4.2 mWm^{-2}) has been determined at DSDP Site 374 (Erickson and Von Herzen, 1978).

The only detail survey has been carried out along two profiles by Della Vedova and Pellis (1989): (a) A transect crossing the VHS (almost coinciding with profile IV of Avedik and Hieke, 1981) shows maximum values of 36.9 ± 4.3 mWm^{-2} (NW) and 36.3 ± 3.5 mWm^{-2}(SE) and a minimum of 30.6 ± 0.6 mWm^{-2} near the rim of VHS and an average observed value of 35.1 ± 2.6 mWm^{-2}. (b) A profile parallel to a seismic line along the Medina Ridge Glacis (Avedik and Hieke, 1981, I and II in fig. 1). Eight

measurements near the western end exhibit an average value of 44.5 ± 2.8 mWm^{-2}, whereas the two measurements located near VHS-2 result in an average value of 34.9 ± 2.2 mWm^{-2} which is consistent with that observed on the VHS profile. A modelling suggests that VHS is in thermal equilibrium with the deep structures.

All reported values are below the mean heat flow for the earth (50–63 mWm^{-2}; Sheriff, 1984). They obviously signalize stable thermal conditions though recent vertical movements are observed in the IAP.

Discussion

The main contrast in the interpretation of the characteristics and the history of the IAP is defined with the question ''Is the IAP a remnant of an old Tethys ocean which opened in Jurassic time, or is it a thinned part of the African continental crust (and Adria is then to be considered as an African promontory)?''

The following discussion will try to find out how the observations can be interpreted and which of the conflicting models of IAP structure and history can be corroborated by them.

Subbottom information

Four types of structural elements observed in the seismic reflection records are conspicuous: (A) antithetical, southeastward (in W–E oriented profiles apparently eastward) dipping pre-Messinian reflectors, (B) domings of pre-Messinian rocks, (C) a non-uniform Plio-Quaternary sequence in the southern IAP, and (D) the ''Undulation Zone'' (Hinz, 1974).

Pre-Messinian, southeastward dipping reflectors

The pre-Messinian reflectors PM2 to PM4 show a pattern of repeated parallel inclinations (tilted blocks). PM1 is sometimes also parallel with the deeper ones (Figures 7–10), sometimes it dips with a smaller angle (Figures 7–9, 11) or even in the opposite direction (Figures 9–11). The BE reflector lies normally almost horizontal except in Figure 7 where it is subparallel with the PMs. These variations result in wedge-like increases of the PM2/PM1 and PM1/BE interval thicknesses (synrift wedges).

The geometry of the PM reflectors signalize that the area was stable up to young pre-Messinian times. Then, the whole area was affected by tectonic deformations. The width of the blocks varies considerably as can be obtained e.g. from Figures 7 and 8 (the horizontal scale is fairly identical).

Domings of pre-Messinian rocks

The domings (see Section ''The Messinian interval'') uncover their internal structures in varying degrees. The most prominent VHStr gives the worst information; reflectors are just indicated if at all. Within NStr, there can be discerned a reflector (PM2?) which is tilted towards the west (Figure 7) as well as towards the east (Figures 8 and 11). VaStr (Figure 7) presents a well developed sequence of three reflectors (PM2, PM2a, PM3) which dip eastward.

The identification of the domings in the respective seismic profiles was made using the VHStr as the guide line because of its great vertical amplitudes which result in seafloor elevations. NStr and VHStr are more or less parallel SW–NE oriented (Figure 2). The domings separate ''basins'' of Messinian evaporites. Their maximum thicknesses increase from SE to NW. The basins must have pre-existed at the beginning of evaporation and have been modified in detail during the Messinian.

A vertical difference of about 0.1 s TWT of the M reflector above NStr indicates post-Messinian movements. VHStr is part of the Medina-Victor Hensen Structure (M-VHStr; Hieke and Dehghani, 1999). The latter is displaced along its course several times vertically (seahills) and horizontally (by left lateral faults) as well. Figure 2 shows a modified course compared with Hieke and Dehghani (1999). The faulting cannot be dated. However, a recent vertical offset of the seafloor is evident above VHStr.

Length and degree of deformation of the domings correlate positively: The most extended M-VHStr is that one most affected by deformation.

There are obviously close relations between the tilted blocks and the domings, as VHStr demonstrates. Where VHStr is only a subbottom structure, it is very similar to NStr. That again is comparable with the unspectacular VaStr. As a consequence, one can consider the domings and the highest parts of the tilted blocks as parts of a

common tectonic pattern with different age of deformation and intensity: The tilting of the blocks happened in pre-Messinian time. Some are inactive since the beginning of the evaporite deposition or became inactive before the end of the Messinian. The domings, originally the risen edges of the rotated blocks, became later the places of normal faults (with a horizontal component?) which did not produce visible vertical rotations. VaStr, NStr and VHStr document (in this order) increasingly longer periods and intensities of deformation as well. Thus, we can deduce that the deformation pattern, characterized by a general SW–NE orientation, has been laid out in pre-Messinian time. Only some of the tectonic elements stayed active in post-Messinian time. Thus, they became the dominating ones (NStr, VHStr).

The continuation of VHStr into the eastern finger of the Medina Ridge is obvious (M-VHStr; Hieke and Dehghani, 1999). A similar but less spectacular situation is supposed to exist north of the central finger of the Medina Ridge (Figure 2), though there is not a clear dominance of the SW–NE orientation of the relief but a mixing with a NW–SE orientation as represented by the Malta Escarpment (insert of Figure 1). A broad and slight doming of BE reflector is recorded on seismic line MS-27 (Finetti 1982, fig. 14, SP 770–790) at about 35°40′N and 17°45′ E. It can be speculated whether it represents the prolongation of the central finger of Medina Ridge.

Reston et al. (2002, fig. 10) have recorded bendings of their reflector B (= BE) which they interpret as folding. It is conspicuous that the bendings do not correspond with those of the overlying reflector M which shows much more bendings. Thus their geometry should have originated independently which contradicts a common folding event. Those few bendings of B might be minor domings compared with VHStr.

None of the subbottom structures show peculiarities of folds as has been assigned to the VHStr by Jongsma et al. (1987).

V-shaped down-bendings of sediments on top of NStr and VaStr (Figures 7–9; Avedik and Hieke, 1981, fig. 10 and 12) may be caused by a combination of post-Messinian faulting and connected subsolution of a thin evaporite cover of the domings (Avedik and Hieke, 1981).

Plio-Quaternary sequence in the southern IAP

The post-Messinian sedimentary filling of IAP is not uniform. Figure 6b demonstrates that the maximum thickness of the pre-STL sequence is situated outside the southern rim of the plain. The STL–TTL interval cannot be observed very well since both reflectors are not identifiable jointly over the whole record. For the post-TTL interval, however, the maximum thickness is recorded beneath the present plain.

According to the turbidite dominance during the Quaternary, we have to explain the situation as follows: During the earlier Plio-Quaternary, the relief was deepest (or the subsidence was highest) near the southern rim of IAP and outside. At a not identifiable time before the sedimentation of TTL (about 650,000 years?), the zone of maximum subsidence shifted towards the north where the present plain is situated. That subsidence is continuing as the concave seafloor indicates.

The Undulation Zone

This occurs generally NW of the domings (i.e. in the area facing the Calabrian Rise) and in part along the rim towards the MR (Figure 2). The undulations affect the complete post-evaporitic sequence in a sector paralleling the rims whereas, with increasing distance from the rims, the undulation effects fade away downwards (Figures 3 and 6c; see also Polonia et al., 2002, profile MS-112 on fig. 4). The occurrence of the Undulation Zone is linked with the shape of the top of evaporites: (1) Above the evaporite basin with the largest width (NW of NStr and VaStr, respectively; Figures 7–9, 11) reflector M is rough. (2) This large basin is that one with the greatest maximum thickness of evaporites. (3) It continues towards the NW under the Calabrian Rise. There, the thickness of evaporites increases though BE reflector is more or less horizontal. Such an increase can be interpreted only by lateral pressure and the resulting plastic evasion of evaporites (incipient diapirism). The effects of these processes do obviously not extend beyond NStr or VaStr towards the SE.

At the MR side of the plain, the situation is more complicated. Along the northern part of the rim, the undulation pattern is almost identical with that on the Calabrian side (affecting

again the evaporite basin with the greatest maximum thickness). In that area, where NStr and VHStr come in contact with the MR deformation front, undulations are almost missing but monoclinal flexures (Figure 3i and k) occur. Further to the south, undulation features occur again (Figure 3j) but less expressed and mixed with flexural ones. Reston et al. (2002, fig. 10) interpreted bendings of the Plio-Quaternary sequence in IMERSE profile 1 (SPs 300-350), which correspond to our Undulation Zone, as folding: The top of Messinian "*appears folded even out in the Messina Abyssal Plain* [=IAP]. *This folding must predate the deposition of the Plio-Quaternary sequence*. (l.c., p. 74)."

From the Medina Ridge side, undulation features are unknown.

The distribution of the Undulation Zone can be explained as follows: The suggested direction of subduction or accretion under the Calabrian Rise is normal to the orientation of the subbottom structures ("domings"). A lateral stress could affect a wide area between the Calabrian Rise and the domings which act as a barrier. The evasion of the evaporates decreased towards the barrier. At the MR side in contrast, the deformation front of the MR accretionary complex as well as the subduction direction are oriented in angles of about 45° to VHStr and NStr. Moreover, the evaporite basin between both structures is of smaller width and maximum thickness as well. This might be the case also for that basin following SE of VHStr. Its southeastern rim is already incorporated into the accretionary complex and, therefore, unknown. This situation should be unfavourable for the unhindered propagation of lateral stress.

Rim features and tectonics

The distribution of the Undulation Zone and other subbottom and bottom features indicate that the rims of the IAP cannot simply be explained as the deformation fronts of accretionary complexes with outward directed upthrow faulting.

Where the undulations reach the seafloor, they cause a small-scaled rough relief ("cobblestones"). This is sometimes arranged in "terraces". At the MR side, the situation shows more variations since, additionally to the pure Calabrian type, also step-like rims (tensional?) occur. It is necessary to interpret the outer boundaries of the Calabrian Rise and the MR (if defined with the rim of IAP) as primarily vertical reactions of the plastic evaporites and not as outermost effects of upthrow faulting (deformation front). Real accretionary shortening may act inside the accretionary complexes in a distance from their morphologically defined outer boundaries.

In contrast, the rim towards the Medina Ridge is characterized by flexures and steps obviously caused by normal faults being common in the Medina Ridge Glacis (Hieke and Dehghani, 1999), which itself seems to be the product of down-faulting compared with the Medina Ridge.

Nature of the crust underneath the Ionian Sea and structural implications

An evaluation of the literature (Hieke and Dehghani, 1999), yielded a wide spectrum of controversial interpretations including oceanic and continental crusts. They can be very roughly categorized as follows (some authors gave ambivalent interpretations):

Continental or thinned continental crust
Finetti and Morelli (1973), Cloetingh et al. (1980), Farrugia and Panza (1981), Baldi et al. (1982), Calcagnile et al. (1982), Mantovani (1982), Mantovani and Boschi (1982), Boccaletti et al. (1984), Makris et al. (1986), Leister et al. (1986), Ferrucci et al. (1991), Cernobori et al. (1996), Mantovani et al. (2002).

Neither typically continental nor typically oceanic crust
Hinz (1974), Weigel (1974), Morelli (1978)

Oceanic or intermediate type of oceanic crust; uplifting of the basement and volcanic activities
Finetti (1981, 1982), Makris et al. (1986), Leister et al. (1986), de Voogd et al. (1992), Finetti et al. (1996), Catalano et al. (2001).

Geological and tectonic maps demonstrate with their inconsistency the scarcity of exact crust data:

– Khain and Leonov (1979): oceanic crust is restricted to the IAP.

– Choubert and Faure-Muret (1987): boundary continental/oceanic crust crosses the Medina Ridge.
– Bogdanov and Khain (1994): the highly elevated Medina Ridge is traversed by the boundary between oceanic crust and a stripe of thinned continental crust which embraces water depths between 3500 and 1000 m.

The geodynamic concept of an Ionian Ocean of Catalano et al. (2001) is based on paleogeographic and plate tectonic considerations in the neighbourhood of the Ionian Sea. There is no new and verifiable information from the Ionian Sea itself. Main arguments are the Malta and Apulia Escarpments which are considered as old conjugating passive margins. From that, the existence of an ocean between them seems inevitably to result. Catalano et al. (2001) continued to find evidence for a (NW–SE trending) midoceanic ridge just in the middle between the passive margins. They found it in their seismic profile C9434 (fig. 6) on the Calabrian Rise with its generally rough topography: An ''anomalous depression'' connected with converging reflectors should be witness for that feature. A look at a modern bathymetric map (e.g. IOC, 1981) or at a multibeam imagery (e.g. Loubrieu et al., 2000) will easily show, how many such ''anomalous depressions'' occur on the Calabrian Rise.

Bosellini (2002) presents strong arguments (different geological history) against the passive margin nature of the apparently ''conjugating'' Malta and Apulia Escarpments. Moreover, from the occurrence of dinosaurs on the Apulia carbonate platform, Bosellini (l.c.) concludes that Apulia was connected to Africa (not separated by deep water) and the Late Jurassic – Early Cretaceous Ionian Sea region was a ''cul-de-sac'' -type basin enclosed by shallow-water carbonate banks.

Hieke and Dehghani (1999) demonstrated that the VHStr is connected with the eastern finger of the Medina Ridge. The resulting ''Medina – Victor Hensen Structure'' (M-VHStr) is at least 155 km long, can be followed to the lower slope of the MR and is intersected by left lateral faults. The Medina Ridge at the southwestern end of the M-VHStr is commonly accepted to be underlain by thinned continental crust (e.g. Finetti, 1982). In the case of Khain and Leonov (1979), the narrow M-VHStr would extend from thinned continental to old oceanic crust surmounting a maximum depth difference of 2500 m. In the cases of Choubert and Faure-Muret (1987) and Bogdanov and Khain (1994) one would have a respective depth difference within an area underlain by oceanic crust.

The VHStr has been considered by several authors to be the continuation of the Cefalonia Fault (Hieke and Dehghani, 1999). That again is interpreted as a long transform fault which easily could run from an oceanic to a (thinned) continental area. However, two facts take the VHStr its value as an unique feature (even if it is the most prominent one) and the considerations on the Cefalonia Fault/VHStr relation become less obtruding: (a) the pattern of several subbottom structures more or less parallel to the VHStr (Figures 7–11) and (b) the piercing of the central finger of the Medina Ridge into the IAP near its western end (Figure 2) which suggests a situation similar to that of the M-VHStr but not so expressed.

The geological and geophysical observations presented by Hieke and Dehghani (1999) and those presented in this paper let tend us to a strongly thinned continental character of the IAP crust.

Peculiarities of the IAP – expressions of its geodynamic history

We can summarize the observations as follows:
– IAP is characterized by a SW–NE trending strong positive gravity anomaly.
– There are no magnetic anomalies indicating large magmatic bodies as supposed by some authors.
– Heat flow is low with minor variations.
– The type of the crust (interpretations based on seismic refraction and Raleigh wave dispersion measurements) is contested (old oceanic, thinned continental, thick continental).
– The deepest recognized seismic reflector lies in a depth of 9 s TWT.
– Most of the pre-Messinian seismic reflectors are parallel and inclined to the southeast.
– The uppermost pre-Messinian reflector interval shows wedge-like thickness variations because of the horizontal position of BE reflector. This dates the vertical rotation of the PM reflectors as mainly pre-Messinian.

- Rotation of the PM reflectors produced some depressions and elevations which are elongated with a SW–NE orientation.
- The depressions have been filled by evaporites during the Messinian (evaporite basins).
- The maximum thicknesses of the evaporite basins increase from SE to NW.
- The elevations (domings of the pre-Messinian) between the basins (VHStr, NStr, VaStr) rise to different levels.
- The most extended of the domings (VHStr) owns the largest vertical differences. It rises at some places above the present seafloor. Its axis is shifted several times by left lateral faults (i.e. clock-wise rotation). The trend of the faults might be about 110–120° as can be constructed between VHS-2 and the Medina Ridge finger.
- Reflector M shows a vertical offset above or on both sides of VHStr and NStr, which indicates post-Messinian tectonics.
- The Plio-Quaternary sedimentary cover shows V-shaped down-bendings above some domings. They are interpreted as the result of a combination of graben-like faulting triggering subsolution of evaporites.
- The drastic change of the facies in the present IAP area at about the Pliocene/Quaternary boundary (normal hemipelagic to turbidite-dominated) might indicate a strong subsidence which gave the relief for turbidite accumulation.
- The thickness of the Plio-Quaternary sequence (which means mainly of the turbidite-dominated Quaternary) is controlled by (a) the subsidence of the respective area and (b) the secondary increase of the thickness of evaporites near the Calabrian Rise.
- Thickness variations within the (Plio-)Quaternary sequence document that the maximum subsidence was located during the pre-STL time near the southern rim of the IAP and changed in post-STL time towards the north.
- Subsidence/vertical tectonics are still active at present time.

These peculiarities provide the following concept of the tectonic and sedimentary evolution of the IAP.

In Mesozoic (and early Tertiary?) time, the area seems to have been tectonically quiescent. Then, the area was broken in elongated blocks of varying widths. They were antithetically tilted (rifting?) during late pre-Messinian times. Declining movements may have continued during the Messinian. A general subsidence, varying in detail, controlled the evaporite thicknesses within basins which were separated by thresholds (the highest parts of the tilted blocks). The alternative idea of a fixed pre-existing relief which has been simply filled during the Messinian evaporation phase is rather unlikely since it would describe a persistence which is not in accordance with the general dynamic situation.

The thresholds (domings) may have been active (relative elevation) also during Messinian time. In any case, normal faulting was active in post-Messinian time (vertical offset of reflector M). Shifting of the place of maximum subsidence from the south to the north and faulting controlled the thickness of Quaternary sediments which mainly consist of turbidites.

The continuation of subsidence and normal faulting up to the present produced the slightly concave seafloor and seafloor steps, which could be soon balanced by the frequent turbidites.

The V-shaped down-bendings of the Plio-Quaternary layers on top of NStr and VaStr are still active. They might be caused by a combination of graben-forming faults on top of a horst and the subsolution of the evaporite cover on the threshold supported by water circulating along faults.

A completely different process caused the decreasing thickness of Quaternary sediments towards the Calabrian Rise rim: the lateral immigration of evaporites from the Calabrian Rise produced a more or less continuous rising of the seafloor and the undulation layering of parts of the plain filling. This process played obviously a minor role on the MR side, where the primary thickness of evaporites is smaller.

IAP in the frame of plate tectonics

Published conceptions of the role of IAP in the plate tectonic history (synopsis see Hieke and Dehghani, 1999) are contrary and supported very differently. Scandone et al. (1981) listed six hypotheses on the origin of the Ionian Basin. All the ideas seem to be based on arguments which cannot be easily disregarded. In this situation, it would be helpful to be able to rule out some of the hypotheses by established facts:

The concept of the occurrence of large volcanic bodies in the IAP (Biju-Duval and Montadert, 1977; Finetti, 1982, Marconi Seamount instead of VHStr) is not valid.

Medina Ridge is not part of a right-lateral wrench zone as postulated by Jongsma et al. (1987). The northern part of the Medina Ridge is characterized by SW–NE and SSE–NNW trending faults. There are no SW–NE trending folds in the IAP. The horizontal offsets of M-VHStr indicate left-lateral faults.

Cephalonia Fault cannot be considered simply as a large SW–NE trending strike-slip fault (it matters little whether left or right lateral) extending to IAP, correlatable with M-VHStr (Della Vedova and Pellis, 1989) or as still separating the Adriatic microplate from the African Plate (Anzidei et al., 1996). M-VHStr is (a) not only a fault but a horst-like elevation of pre-Messinian rocks and (b) intersected by SE–NW trending left-lateral faults.

Active subduction of IAP under the Calabrian Arc is not well proved by data (Mantovani et al., 1985, p. 69). The upper part of the Calabrian Rise consists of chaotic masses (Rossi and Sartori, 1981; Morlotti et al., 1984) which may have slumped from the Calabrian Arc which underwent a considerable uplift since Pliocene time (Ghisetti and Vezzani, 1982). The lower slope of the Calabrian Rise and its detailed relief are determined by the secondary increase of the thickness of evaporites which were squeezed towards the Ionian foreland. The evaporite migration caused the diapir-like undulations of the covering Plio-Quaternary sediments.

The tectonic activities we obtained from the seismic records of IAP start in late pre-Messinian times. That means they are mainly contemporaneous with the opening of the Tyrrhenian Basin. Therefore, it suggests itself to consider the history of IAP since late pre-Messinian times in very close connection with that of the Tyrrhenian. The causes for the opening of the Tyrrhenian have been discussed by Calcagnile et al. (1981) and Mantovani et al. (1990). Sartori (1990) has described the tectonic history of the Tyrrhenian Sea and peri-Tyrrhenian areas based on the results of ODP Leg 107. From Sartori's diction one could get the impression that the rifting in the Tyrrhenian Sea caused the anticlockwise rotation of the Apennines (and implicitly of the Adriatic block). Mantovani et al. (1990) presented the hypothesis that the opening of the Tyrrhenian was caused by the anticlockwise rotation of the Adriatic block which was always in connection with the African Plate. Driving force for the rotation was the northeastward push of Africa against Adria.

Malinverno and Ryan (1986) characterized in their concept of the extension of the Tyrrhenian Sea the area between the present Malta and Apulian Escarpments as "deep basin in the Africa-Adriatic domain" (fig. 10). The authors abstain from identifying that domain as an oceanic realm, following the arguments of D'Argenio et al. (1980) for the post-Triassic evolution of the Tethyan continental margin in the Apennines and in Sicily-North Africa. Malinverno and Ryan suggested that the Ionian Sea crust (thinned continental or possibly oceanic) is involved in the subduction. This suggestion is based on the considerations of Molnar and Gray (1979) that continental lithosphere can theoretically be subducted if it is pulled into the asthenosphere by oceanic lithosphere coupled to it, and/or if the continental crust is thin enough.

The model of Malinverno and Ryan (1986) has some similarity with the suggestion of Leister et al. (1986) that the Ionian Sea crust is stretched continental and that a very old passive margin was subjected to subsidence over large periods.

We are far from a clear concept of how to integrate the IAP scenario, which we deduced from our inventory, into the hypothesis of Mantovani et al. (1990). However, we believe that this hypothesis is the right way to find an explanation for what happened in this relatively small but very complicated area, instead of those models which operate with IAP as a remainder of the Jurassic Tethys.

The Malta Escarpment has been considered by Carbone et al. (1984) to be rejuvenated and by Scandone et al. (1981) to be not necessarily coinciding with a continent–ocean transition. The correspondence of the orientations of Malta Escarpment and of internal structures of the western part of Medina Ridge is obvious. The eastern part of the Medina Ridge is dominated by the SW–NE orientation which is also characteristic for the subbottom structures of IAP. M-VHStr demonstrates a direct structural con-

nection between Medina Ridge and IAP. Mantovani et al. (1997) assume a clockwise rotation and westward motion of the "Southern Adriatic Plate" which is allowed by a left lateral shear zone (Medina Ridge) decoupling the Adriatic/Northern Ionian area from northnortheast-ward drifting Africa. This concept is indeed in contrast to the interpretation of Medina Ridge as a right lateral wrench zone (Jongsma et al., 1987), but fits well with our observation of the left lateral shearing of M-VHStr.

Many questions are still open. For example what was the stress field which caused the SE dipping pre-Messinian blocks? Why is IAP characterized by very low heat flow, though the plain is affected by young faulting and subsidence?

We will leave the stage of hypotheses and arrive at the stage of a well founded concept for the history of the central Ionian Sea not by speculations and extrapolations but only by collecting more data from the area itself and its neighbourhood.

Acknowledgements

We acknowledge the work and help of the captains, ship's and scientific crews of the cruises Meteor 50 (1978), Valdivia 120 (1992), Meteor 25/4 (1993) and Meteor 40/1 (1997). We are also grateful to K. Hinz and F. Fabricius as well as Woods Hole Oceanographic Institution for making available unpublished data, K. Brodbeck for computer assistance, J. Hartmann for processing of seismic data. M.B. Cita and two anonymous reviewers gave helpful comments.

Notes

[1]All water depths without indication are uncorrected with regard to the sound velocity.

[2]Recorded differences on crossings of Parasound and older records: Track 513 (Parasound) with 3978 m versus track 910 (Meteor 50, 1978) with 3970 m; track 513 (Parasound) with 3979 m versus track 1.7 (Valdivia 120, 1992) with 3971 m. Comparisons between Parasound and Sonne 30 data show that the Sonne 30 depths are 10–11 m less than those of Parasound. Therefore, it seems to be justified to correct the depths of cruises Meteor 17, Meteor 50 and Valdivia 120 by addition of 8 m and the Sonne 30 depths by addition of 11 m.

References

Anzidei, M., Baldi, P., Casula, G., Crespi, M. and Riguzzi, F., 1996, Repeated GPS surveys across the Ionian Sea: evidence of crustal deformations, *Geophys. J. Int.* **127**, 257–267.

Avedik, F. and Hieke, W., 1981, Reflection seismic profiles from the central Ionian Sea (Mediterranean) and their geodynamic interpretation, "*Meteor" Forsch.-Ergebnisse* **C 34**, 49–64.

Baldi, P., Degli Angioli, E., Piallini, L. and Mantovani, E., 1982, Gravity anomaly interpretation in the Calabrian Arc and surrounding regions: a tridimensional approach, *Earth Evol. Sci.* **3**, 243–247.

Biju-Duval, B. and Montadert, L., 1977, Introduction to the structural history of the Mediterranean basins, in Biju-Duval, B. and Montadert, L. (eds.), Structural History of the Mediterranean Basins (Sympos. Split 1976), Paris (Editions Technip), pp. 1–12.

Biju-Duval, B., Dercourt, J. and Le Pichon, X., 1977, From the Tethys Ocean to the Mediterranean Seas: a plate tectonic model of the evolution of the western Alpine system, in Biju-Duval, B. and Montadert, L. (eds.): Structural History of the Mediterranean Basins (Sympos. Split 1976), Paris (Editions Technip), pp. 143–164.

Biju-Duval, B., Morel, Y., Baudrimont, A., Bizon, G., Bizon, J.J., Borsetti, A.M., Burollet, P.F., Clairefond, P., Clauzon, G., Colantoni, P., Mascle, G., Montadert, L.. Perrier, R., Orsolini, P., Ravenne, C., Taviani, M. and Winnock, E., 1982, Donnés nouvelles sur les marges du bassin Ionien profond (Méditerranée Orientale). Résultats des campagnes Escarmed, *Revue Inst. Franç. Pétrole* **37**, 713–731.

Boccaletti, M., Nicolich R., and Tortorici, L., 1984, The Calabrian Arc and the Ionian Sea in the dynamic evolution of the Central Mediterranean, *Mar. Geol.* **55**, 219–245.

Bogdanov, N.A. and Khain, V.E. (eds.), 1994, Tectonic Map of the Mediterranean Sea, 1:5,000,000, Institute of Lithosphere, Academy of Sciences of Russia, Moscow.

Bosellini, A. (2002), Dinosaurs "re-write" the geodynamics of the eastern Mediterranean and the paleogeography of the Apulia Platform, *Earth-Sci. Rev.* **59**, 211–234.

Calcagnile, G., Fabbri, A., Farsi, F., Gallignani, P., Gasparini, C., Iannacone, G., Mantovani, E., Panza, G.F., Sartori, R., Scandone, P. and Scarpa, R., 1981, Structure and evolution of the Tyrrhenian basin, *Rapp. Comm. int. Mer Médit.* **27**(8), 197–208.

Calcagnile, G., D'Ingeo, F., Farrugia, P. and Panza, G.F., (1982), The lithosphere in the Central-eastern Mediterranean area, *Pageoph.* **120**, 389–406.

Carbone, S., Grasso, M. and Lentini, F., 1984, Considerazioni sull'evoluzione geodinamica della Sicilia sud-orientale dal Cretaceo al Quaternario, *Mem. Soc. Geol. It.* **24**(1982), 367–386.

Carter, T.G., Flanagan, J.P., Jones, C.R., Marchant, F.L., Murchinson, R.R., Rebman, J.H., Sylvester, J.C., and

Whitney, J.C., 1971, A new bathymetric chart and physiography of the Mediterranean Sea, in Stanley, D.J. (ed.), The Mediterranean Sea: A Natural Sedimentation Laboratory. Dowden, Hotchinson and Ross, (Stroudsburg, Pa.), pp. 1–23.

Casero, P., Cita, M.B., Croce, M., and De Micheli, A., 1985, Tentativo di interpretazione evolutiva della scarpata di Malta basata su dati geologici e geofisici, *Mem. Soc. Geol. It.* **27**, 233–253.

Catalano, R., Franchino, A., Merlini, S. and Sulli, A., 2000: A crustal section from the Eastern Algerian basin to the Ionian ocean (Central Mediterranean), *Mem. Soc. Geol. It.* **55**, 71–85.

Catalano, R., Doglioni, C. and Merlini, S., 2001, On the Mesozoic Ionian Basin, *Geophys. J. Int.* **144**, 49–64.

Čermak, V. and Hurtig, E., 1979, Heat Flow map of Europe, 1: 5,000,000, in Čermak, V. and Rybach, L. (eds.), *Terrestrial Heat Flow in Europe*, Springer, Berlin, Heidelberg, New York.

Cernobori, L., Hirn, A., McBride, J.H., Nicolich, R., Petronio, L., Romanelli, M. and Streamers/ Profiles Working Groups, 1996, Crustal image of the Ionian Basin and its Calabrian margins, *Tectonophysics* **264**, 175–189.

Choubert, G. and Faure-Muret, A., 1987, International Geological Map of Africa, 1:5,000,000, sheet 2, Commission of the Geological Map of the World.

Cita, M.B. and Aloisi, G., 2000, Deep-sea tsunami deposits triggered by the explosion of Santorini (3500 y BP), eastern Mediterranean, *Sed. Geol.* **135**, 181–203.

Cita, M.B., Ryan, W.B.F., and Kidd, R.B., 1978, Sedimentation rates in Neogene deep-sea sediments from the Mediterranean and geodynamic implications of their changes, in Hsü, K.J., Montadert, L. et al., *Init. Rep. DSDP* **XLII**, (part 1) 991–1002.

Cita, M.B., Camerlenghi, A., Kastens, K.A., and McCoy, F.W., 1984, New findings of Bronze Age homogenites in the Ionian Sea: geodynamic implications for the Mediterranean, *Mar. Geol.* **55,** 47–62.

Cloetingh, S., Nolet, G. and Wortel, R., 1980, Crustal structure of the Eastern Mediterranean inferred from Rayleigh wave dispersion, *Earth Planet. Sci. Letters* **51**, 336–342.

D'Argenio, B., Horváth, F. and Channel. J.E.T., (1980), Palaeotectonic evolution of Adria, the African promontory, in Aubouin, J, Debelmas, J, and Latreille, M. (eds.), Géologie des chaîne alpines issue de la Tethys, *Mém. B.R.G.M.* **115**, 331–351.

Della Vedova, B. and Pellis, G., 1989, New heat flow density measurements in the Ionian Sea, *CNR, Gruppo Naz. di Geofisica della Terra Solida, Atti dell'8o Conv.* **II**, 1133–1146.

De Voogd, B., Truffert, C., Chamot-Rooke, N., Huchon, P., Lallemant, S., and Le Pichon, X., 1992, Two-ship deep seismic soundings in the basins of the Eastern Mediterranean Sea (Pasiphae cruise), *Geophys. J. Int.* **109,** 536–552.

Erickson, A.J., Simmons, G., and Ryan, W.B.F., 1977, Review of heatflow data from the Mediterranean and Aegean Seas, in Biju-Duval, B. & Montadert, L. (eds.), Structural History of the Mediterranean Basins (Sympos. Split 1976), Paris (Editions Technip), 263–280.

Erickson, A.J. and Von Herzen, R.P., 1978, Down-hole temperature measurements, Deep Sea Drilling Project, Leg 42A, in Hsü, K.J., Montadert, L. et al., *Init. Rep. DSDP* **XLII**, (part 1), 857–871; Washington.

Farrugia, P. and Panza, G.F., 1981, Continental character of the lithosphere beneath the Ionian Sea, in Cassinis, R. (ed.), The Solution of the Inverse Problem in Geophysical Interpretation. Plenum Press, New York and London, pp. 327–334.

Ferrucci, F., Gaudiosi, G., Hirn, A. and Nicolich, R., 1991, Ionian Basin and Calabrian Arc; Some new elements from DSS data, *Tectonophysics* **195**, 411–419.

Finetti, I., 1981, Geophysical study on the evolution of the Ionian Sea, in Wezel, F.C. (ed.), Sedimentary basins of Mediterranean margins. C.N.R. Italian Project of Oceanography, Bologna (Tecnoprint), pp. 465–484.

Finetti, I., 1982, Structure, stratigraphy and evolution of Central Mediterranean, *Boll. Geofis. Teor. Appl.* **24**, 247–312.

Finetti, I. and Morelli, C., 1972, Wide scale digital seismic exploration of the Mediterranean Sea, *Boll. Geofis. Teor. Appl.* **14**, 291–341.

Finetti, I. and Morelli, C., 1973, Geophysical exploration of the Mediterranean Sea, *Boll. Geofis. Teor. Appl.* **15**, 263–341.

Finetti, I., Lentini, F., Carbone, S., Catalano, S. and Del Ben, A., (1996), Il sistema Appennino meridionale – Arco Calabro – Sicilia nel Mediterraneo centrale: studio geologico-geofisico, *Boll. Soc. Geol. It.* **115**, 529–559.

Ghisetti, F. and Vezzani, L., 1982, The recent deformation mechanism of the Calabrian Arc, *Earth Evol. Sci.* **3**, 197–206.

Hartmann, J., 1995, Geophysikalische Untersuchungen in der Ionischen See, Berichte aus dem Zentrum für Meeres- und Klimaforschung, Reihe C, **10**. Hamburg.

Hieke, W., 1978, The "Victor Hensen Seahill"; part of a tectonic structure in the central Ionian Sea, *Mar. Geol.* **26**, M1–M5.

Hieke, W., 1984, A thick Holocene homogenite from the Ionian Abyssal Plain (Eastern Mediterranean), *Mar. Geol.* **55**, 63–78.

Hieke, W., 2000, Transparent layers in seismic reflection records from the central Ionian Sea (Mediterranean) – evidence for repeated catastrophic turbidite sedimentation during the Quaternary, *Sediment. Geol.* **135**, 89–98.

Hieke, W. and Dehghani, G.A., 1999, The Victor Hensen Structure in the central Ionian Sea and its relation to the Medina Ridge (Eastern Mediterranean), *Z. dt. geol. Ges.* **149**, 487–505.

Hieke, W. and Wanninger, A., 1985, The Victor Hensen Seahill (central Ionian Sea) – morphology and structural aspects, *Mar. Geol.* **64**, 343–350.

Hieke, W. and Werner, F., 2000, The Augias megaturbidite in the central Ionian Sea (Central Mediterranean) and its relation to the Holocene Santorini event, *Sediment. Geol.* **135**, 205–218.

Hieke, W., Hirschleber, H.B., and Dehghani, G.A., 1998, The crust of the Ionian Abyssal Plain – old oceanic?, *Rapp. Comm. int. Mer Médit.* **35**, 72–73.

Hinz, K., 1974, Results of seismic refraction and seismic reflection measurements in the Ionian Sea, *Geol. Jb.* **E 2,** 33–65.

Hirschleber, H.B., Hartmann, J.M. and Hieke, W.,1994, The Mediterranean Ridge accretionary complex and its forelands - seismic reflection studies in the Ionian Sea, in Ansorge, R. (ed.), Universität Hamburg 1994 – Schlaglichter der Forschung zum 75. Jahrestag. Hamburger Beiträge zur Wissenschaftsgeschichte **15**, Reimer-Verlag Berlin/Hamburg, pp. 491–509.

Hsü, K.J., Montadert, L., Bernoulli, D., Bizon, G., Cita, M.B., Erickson, A., Fabricius, F., Garrison, R.E., Kidd, R.B., Mélières, F., Müller, C. and Wright, R.C., 1978, Site 374:

Messina Abyssal Plain, in Hsü, K.J., Montadert, L. et al., *Init. Rep. DSDP* **XLII**, (part 1) 175–217.

IHO/IOC, 1990, List of geographical names of undersea features shown (or which might be added) on the International Bathymetric Chart of the Mediterranean (IBCM), and on the IHO small-scale international chart series, for the Mediterranean. Edited by International Hydrographic Organization/Intergovernmental Oceanographic Commission, 1st ed., Monaco 1990.

IOC – Intergovernmental Oceanographic Commission, 1981, International Bathymetric Chart of the Mediterranean, 1 : 1,000,000 (Lat. 38°). 10 sheets. Head Department of Navigation Oceanogr., Leningrad.

IOC – Intergovernmental Oceanographic Commission, 1989, Bouguer Gravity Anomalies (IBCM-G). International Bathymetric Chart of the Mediterranean, Geological–Geophysical Series, 1 : 1,000,000 (Lat. 38°). 10 sheets. Leningrad (Head Department of Navigation Oceanogr.).

IOC – Intergovernmental Oceanographic Commission, 2000, Magnetic Anomalies (IBCM-M). International Bathymetric Chart of the Mediterranean, Geological–Geophysical Series, 1 : 1,000,000 (Lat. 38°). 10 sheets. Leningrad (Head Department of Navigation Oceanogr.).

Jongsma, D., Woodside, J.M., King, G.C.P. and van Hinte, J.E., 1987, The Medina Wrench: a key to the kinematics of the central and eastern Mediterranean over the past 5 Ma., *Earth Planet. Sci. Lett.* **82**, 87–106.

Kastens, K.A. and Cita, M.B. 1981, Tsunami-induced sediment transport in the abyssal Mediterranean Sea, *Geol. Soc. Amer. Bull.* **92(**Part I), 845–857.

Kastens, K.A., Breen, N.A. and Cita, M.B., 1992, Progressive deformation of an evaporite-bearing accretionary complex: SeaMARC I, SeaBeam and piston-core observations from the Mediterranean Ridge, *Marine Geophys. Res.* **14,** 249–298.

Khain, V. and Leonov, Yu. (eds.), 1979, Carte tectonique de l'Europe et des régions avoisantes, 1:10,000,000, Commission de la Carte géologique du Monde.

Leister, K., Makris, J., Nicolich, R. and Ramcke, D, 1986, Crustal structure and crustal development in the Ionian Sea, *Rapp. Comm. int. Mer Médit.* **30**(2), 84.

Loubrieu, B., Satra, C. and Cagna, R. 2000, Cartographie par sondeur multifaisceaux de la Ride Méditerranéenne et des domains voisins. – Editions Ifremer.

Makris, J. and Stobbe, C., 1984, Physical properties and state of the crust and Upper Mantle of the Eastern Mediterranean Sea deduced from geophysical data, *Mar. Geol.* **55**, 347–363.

Makris, J., Nicolich, R. and Weigel, W., 1986, A seismic study in the western Ionian Sea, *Annales Geophysicae* **4B**, 665–678.

Malinverno, A. and Ryan, W.B.F., 1986, Extension in the Tyrrhenian Sea and shortening in the Apennines as result of arc migration driven by sinking of the lithosphere, *Tectonics* **5**(2), 227–245.

Mantovani, E., 1982, Some remarks on the driving forces in the evolution of the Tyrrhenian Basin and Calabrian Arc, *Earth Evol. Sci.* **3**, 266–270.

Mantovani, E. and Boschi, E.. 1982, Short period Raleigh wave dispersion in the Calabrian Arc and surrounding regions, *Earth Evol. Sci.* **3**, 239–242.

Mantovani, E., Babbucci, D. and Farsi, F., 1985, Tertiary evolution of the Mediterranean region: major outstanding problems, *Boll. Geofis. Teor. Appl.* **26,** 67–90.

Mantovani, E., Babucci, D., Albarello, D. and Mucciarelli, M., 1990, Deformation pattern in the central Mediterranean and behavior of the African/Adriatic promontory, *Tectonophysics* **179**, 63–79.

Mantovani, E., Albarello, D., Tamburelli, C., Babbucci, D. and Viti, M., 1997, Plate convergence, crustal delamination, extrusion tectonics and minimization of shortening work as main controlling factors of the recent Mediterranean deformation pattern, *Annali di Geofisica* **XL**, 611–643.

Mantovani, E., Albarello, D., Babbucci, D., Tamburelli, C. and Viti, M., 2002, Trench-arc-back arc systems in the Mediterranean area: examples of extrusion tectonics, *J. Virtual Explorer* (online) **8**, 131–147. [http://virtualexplorer.com.au]

Molnar, P. and Gray, D., 1979, Subduction of continental lithosphere: some constraints and certainties, *Geology* **7**, 58–62.

Montadert, L., Letouzey, J., and Mauffret, A., 1978, Messinian event: seismic evidence, in Hsü, K.J., Montadert, L. et al., *Init. Rep. DSDP* **XLII**, (part 1), 1037–1050.

Morelli, C., 1978, Eastern Mediterranean: geophysical results and implications, *Tectonophysics* **46**, 333–346.

Morelli, C., Gantar, G., and Pisani, M., 1975, Bathymetry, gravity and magnetism in the Strait of Sicily and in the Ionian Sea, *Boll. Geofis. Teor. Appl.* **17**, 39–58.

Morlotti, E., Sartori, R., Torelli, L., Barberi, F. and Raffi, I., 1984, Chaotic deposits from the External Calabrian Arc (Ionian Sea, Eastern Mediterranean), *Mem. Soc. Geol. It.* **24** (1982), 261–275.

Mueller, S., 1977, A new model of the continental crust, in Heacock, J.G. (ed.), The Earth's Crust. *Geophys. Monogr. Series* **2**, 289–317.

Müller, J., Hieke, W. and Fabricius, F., 1978, Turbidites at Site 374: their composition, provenance and paleobathymetric significance, in: Hsü, K.J., Montadert, L. et al., *Init. Rep. DSDP* **XLII**, (part 1), 397–400.

Pfannenstiel, M., 1960a, Carte éditée par l'Institut Océanographique et Musée de Monaco d'apres les sondages les plus récents et établie d'apres les sondages publiés par the Hydrographic Office, Washington, D.C., le Bureau Hydrographique International Monaco, les campagnes de l'ALBATROS 1947/48, de la CALYPSO 1955, de la VEMA 1956; 1 : 769 231, no. 8 et 9-Annexe Bull. Inst. Océanogr. Monaco.

Pfannenstiel, M., 1960b, Erläuterungen zu den bathymetrischen Karten des östlichen Mittelmeeres, *Bull. Inst. Océanogr. Monaco* **57**(1192), 60 p.

Polonia, A., Camerlenghi, A., Davey, F. and Storti, F., 2002, Accretion, structural style and syn-contractional sedimentation in the Eastern Mediterranean Sea, *Mar. Geol.* **186,** 127–144.

Reston, T.J., von Huene, R., Dickmann, T., Klaeschen, D. and Kopp, H., 2002, Frontal accretion along the western Mediterranean Ridge: the effect of Messinian evaporites on wedge mechanics and structural style, in Westbrook, G.K. and Reston T.J. (eds.), The Accretionary Complex of the Mediterranean Ridge: Tectonics, fluid flow and the formation of brine lakes, *Mar. Geol.* **186**, 59–82.

Rossi, S. and Sartori, R., 1981, A seismic reflection study of the external Calabrian Arc in the northern Ionian Sea (Eastern Mediterranean), *Marine Geophys. Res.* **4**, 403–26.

Ryan, W.B.F. and Heezen, B.C., 1965, Ionian Sea submarine canyons and the 1908 Messina turbidity current, *Geol. Soc. Am. Bull.* **76**, 915–932.

Ryan, W.B.F., Stanley, D.J., Hersey, J.B., Fahlquist, D.A. and Allan, T.D., 1970, The tectonics and geology of the Mediterranean Sea, in Maxwell, A.E. (ed.), *The Sea*, vol. 4, pt. 2, pp. 387–492, Wiley-Interscience New York.

Sartori, R., 1990, The main results of ODP Leg 107 in the frame of Neogene to Recent Geology of peri-Tyrrhenian areas in: Kastens, K.A., Mascle, J. et al., *Proc. ODP, Sci. Results* **107**, 715–730.

Scandone, P., Patacca, E., Radoicic, R., Ryan, W.B.F., Cita, M.B., Rawson, M., Chezar, H., Miller, E., McKenzie, J. and Rossi, S., 1981, Mesozoic and Cenozoic rocks from Malta Escarpment (Central Mediterranean), *Amer. Assoc. Petrol. Geol. Bull.* **65**, 1299–1319.

Sheriff, R.E., 1984, *Encyclopedic dictionary of exploration geophysics,* Soc. Explor. Geophysicists, Tulsa.

Vogt, P.R. and Higgs, R.H., 1969, An aeromagnetic survey of the eastern Mediterranean Sea and its interpretation, *Earth Planet. Sci. Letters* **5**, 439–448.

Weigel, W., 1974, Die Krustenstruktur unter dem Ionischen Meer nach Ergebnissen refraktionsseismischer Messungen auf den Fahrten 17 und 22 des Forschungsschiffes "METEOR", *Hamburger Geophysikalische Einzelschriften* **26**.

Weigel, W., 1978, A tectonic model of the northern Ionian Sea from refraction seismic data, in Closs, H., Roeder, D. and Schmidt, K. (eds.), Alps, Apennines, Hellenides. Geodynamic investigation along Geotraverses by an International Group of Geoscientists, *Inter-Union Comm. Geodyn., Sci. Rep.* **38**, 328–329.